Chapter 7

ANALYSIS OF CLOUDS WITH AID OF RAOBS

7.1. Why the Raob is Important in Routine Synoptic Cloud Analysis. The cloud observations regularly available to forecasters in surface synoptic reports leave much to be desired as a basis for cloud forecasting. Some of their limitations may be noted:

a. Middle and high clouds are usually only observed and reported when visible from the ground. No heights are given in the synoptic reports, nor are amounts specifically reported, though they may sometimes be estimated from the amounts of low cloud and total cloud cover. In hourly reports, heights and amounts are sometimes estimated or obtained from aircraft.

b. At nighttime, reports of middle and high clouds (height, amount, and type) are less reliable than in daytime.

c. Cloud systems which have portions extending above 15,000 feet are usually associated with frontal systems and/or mid-tropospheric troughs and lows. Their central portions frequently have precipitation falling out of them, accompanied by abundant low clouds; here we usually get no direct information about how high the clouds extend. Only in the fringe area of the cloud systems, where the middle and high clouds often extend beyond the low clouds, are the middle and high clouds directly accessible to observation from the ground.

d. Tops of convective clouds are not reported either, except from a casual aircraft or radar observation. However, from the types of clouds reported and from the type and intensity of the precipitation falling from them, a rough estimate of tops can be obtained in many cases. Knowledge of the local or regional weather regime is important, of course, for this estimate. For example, typical cumulus congestus at 60°N in wintertime may have a vertical extent of 6000 to 8000 feet; in the tropics, of 15,000 to 20,000 feet. Radar reports in the neighborhood often permit a close determination of the tops of convective clouds. Aircraft reports, particularly from aircraft flying in the middle levels are the most reliable.

e. CPS-9 and other radar installations can provide much useful information, particularly on the height of convective cloud, but the radar echo does not necessarily indicate the extent of the visible cloud. (See AWS TR 184.)

f. Vertical-beam radar installations (such as the TPQ-11 now being introduced) would provide a powerful aid in determining the vertical extent of clouds. At the present time, however, only a few sets have been put in operation. We can expect that through research the records from these sets in time will provide much information on cloud structures, but as yet little information is available for operational use. If a dense network of TPQ-11's were available, the task of cloud forecasting, at least for short periods, would be much lessened. (Use of TPQ-11 for cloud interpretation is explained in AWS TR 180 and further reports are in preparation.)

Radiosondes which penetrate cloud-systems reflect to some extent (primarily in the humidity trace) the vertical distribution of clouds. If the humidity element were perfect, there would usually be no difficulties in locating cloud layers penetrated by the sonde. Because of shortcomings in the instrument, however, the relationship between indicated humidity and cloud is far from definite, and an empirical interpretation is necessary. Nevertheless, radiosonde reports give valuable evidence which, when sifted with other available information, aids greatly in determining a coherent picture at least of

stratiform and frontal cloud distributions. Their value in judging air-mass cumulus and cumulonimbus distribution is negligible, however.

7.2.0 Frontal Cloud Structure. A wealth of experience regarding cloud structures of fronts has been collected by meteorologists engaged in aviation forecasting, mainly through debriefing of flight crews. Very little of this experience has been summarized and presented in the form of scientific papers, although the consensus appears to be that frontal cloud is usually layered, that the high cloud is usually detached from the middle cloud, and that middle cloud is often well layered and many times does not extend very high [19] .

Only a few papers contain any statistical summaries which allow an assessment of a "typical" cloud structure with respect to features such as the type of front, distance from the depression center, and geographical area. Some of these papers [41] [42] [56] [57] are discussed in succeeding paragraphs.

Sawyer [56] investigated the cloud structure of 23 fronts over England or vicinity, based on data from the Meteorological Research Flight. He found that the cloud structure is variable. The main frontal cloud masses were usually formed within the warm air mass and extended into the transition zone by evaporation and recondensation of rain or snow. An example of such a situation is shown in Figure 53 and Figures 58a and 58b. The cross-section in Figure 53 shows the cloud mass of the warm front tilting much more steeply than the frontal zone. The thick frontal cloud does not extend much beyond the forward edge of the precipitation area at the surface. Ahead of the precipitation area at the surface, the frontal zone above 800 mb to 700 mb is very dry. These are features found in many fronts, particularly warm fronts.

7.2.1. Warm Fronts. The probability of encountering cloud at any point in the region of an active warm front is shown in Figure 59, which is based on data published by Sawyer and Dinsdale [57]. The frequencies of cloud occurrence were based on 69 active warm fronts over Southern England. (An active warm front was defined as one having a rain belt at least 50 miles wide. The dimensions and slope of the schematic frontal zone were based on average values for the sample.) We notice again that the "ridge" in the probability pattern, coinciding with the locations of highest incidence of cloud, slopes upwards to the right more steeply than the frontal zone. Again, we notice that the frontal zone above about 10,000 feet is relatively cloud-free.

The authors [57] attempted to correlate the thickness of the cloud mass in active warm fronts with the following quantities:

a. Slope of warm boundary.
b. Thickness of frontal zone.
c. Horizontal gradient of potential wet-bulb temperature.
d. Change of geostrophic wind across the surface front.
e. Six-hour change of parameter "d".
f. Change (across the front) of wind component parallel to surface front.
g. Change (across the front) of wind component normal to surface front.

Parameters "a" through "f" showed no correlation with frontal cloud but "g" gave a slight correlation, $r = 0.16$.

7.2.2. Cold Fronts. Cold fronts appear to be just as elusive as warm fronts when it comes to "pinning down" the weather activity at the front by parameters that would characterize the front on the synoptic chart (other than the weather itself).

Austin and Blackmer [5] investigated by radar the precipitation patterns associated with warm-season cold fronts passing Boston, Mass., (30 cases). The fronts were divided into four main types, primarily according to their orientation. Other characteristics chosen to describe the fronts synoptically were:

a. 700-mb temperature contrast across the front.

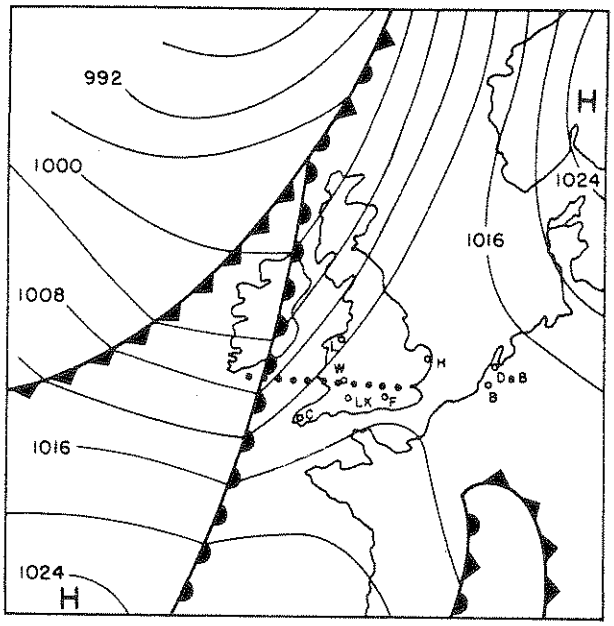

Figure 58a. Surface Chart, 1500 GMT, 19 March 1952. Dotted line indicates vertical plane of the cross-section shown in Figure 53.

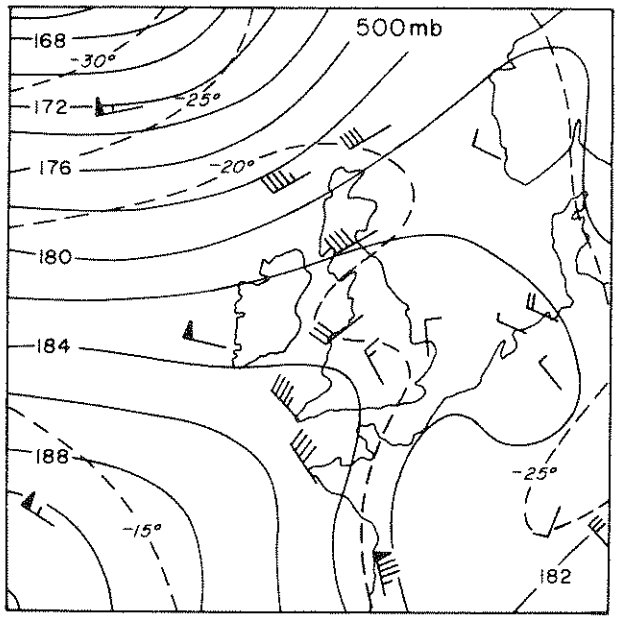

Figure 58b. 500-mb Chart, 1500 GMT, 19 March 1952.

b. Algebraic difference between 2-hour sea-level pressure tendencies before and after frontal passage.

c. 700-mb wind speed and direction immediately ahead of a front.

d. Stability of the warm air (850-mb temperature minus 500-mb temperature).

e. Potential stability of the warm air (850-mb minus 500-mb wet-bulb potential temperature).

f. 850-mb dew-point depression in the warm air.

g. Thermal advection, expressed as $\mathbf{k} \cdot \mathbf{V}_{500\ mb} \times \mathbf{V}_{850\ mb}$, where $\mathbf{k}$ is the vertical unit vector in the warm air.

Neither the orientation classification nor the seven parameters listed above showed any significant relationship to the areal extent of the precipitation.

The precipitation areas, as they appeared on the radar scope, could be described as having three different structures: Isolated showers, bands, or masses. The distribution of these structures with respect to the front is given in Table 4. The highest frequency (23 out of 30 cases) is attached to "no postfrontal precipitation." The next highest is attached to "frontal and prefrontal bands of precipitation." Table 4 confirms the classical picture of the cloudiness extending in bands along or ahead of the cold front and usually breaking up behind the cold front, but it also points out that isolated showers occur nearly as frequently at, ahead of, and behind the front. The absence of postfrontal bands is particularly significant.

Table 5 gives the frequency of occurrence of precipitation as prefrontal, frontal, postfrontal, or combinations thereof, irrespective of structure. We notice the high incidence (30%) of frontal and prefrontal precipitation.

This study stresses the need for considering each cold front individually and finding its characteristics as revealed by the surface observations (clouds, precipitation) and

TABLE 4

Structure of Precipitation Areas Associated with April-September Cold Fronts Near Boston, Mass.

	Number of Cases			
	Frontal	Prefrontal	Postfrontal	Total
Bands	13	9	0	22
Masses	4	6	3	13
Showers	5	8	4	17
None	8	7	23	--
Total	30	30	30	--

TABLE 5

Percentage of Cold Fronts with Specific Precipitation Distribution (irrespective of structure), 30 Fronts, April-September, Boston, Mass.

	Percentage
Frontal Only	13
Prefrontal Only	23
Postfrontal Only	3
Frontal and Prefrontal	30
Frontal and Postfrontal	13
Prefrontal and Postfrontal	7
Frontal, Prefrontal, and Postfrontal	10

raobs, rather than forming a stereotyped picture of weather associated with the blue line on the chart. It is evident that the raobs spaced at 100 to 200 miles can easily give a misleading impression as to the cold-frontal cloud distribution, depending on whether the raobs happened to penetrate a band or cell or a "thin" area.

7.2.3. The Humidity Field in the Vicinity of Frontal Clouds. Figure 53 shows a tongue of dry air extending downward in the vicinity of the front and tilted in the same direction as the front. Sawyer [56] found that such a dry tongue was more or less well developed for all the frontal regions he investigated. This dry tongue was best developed near

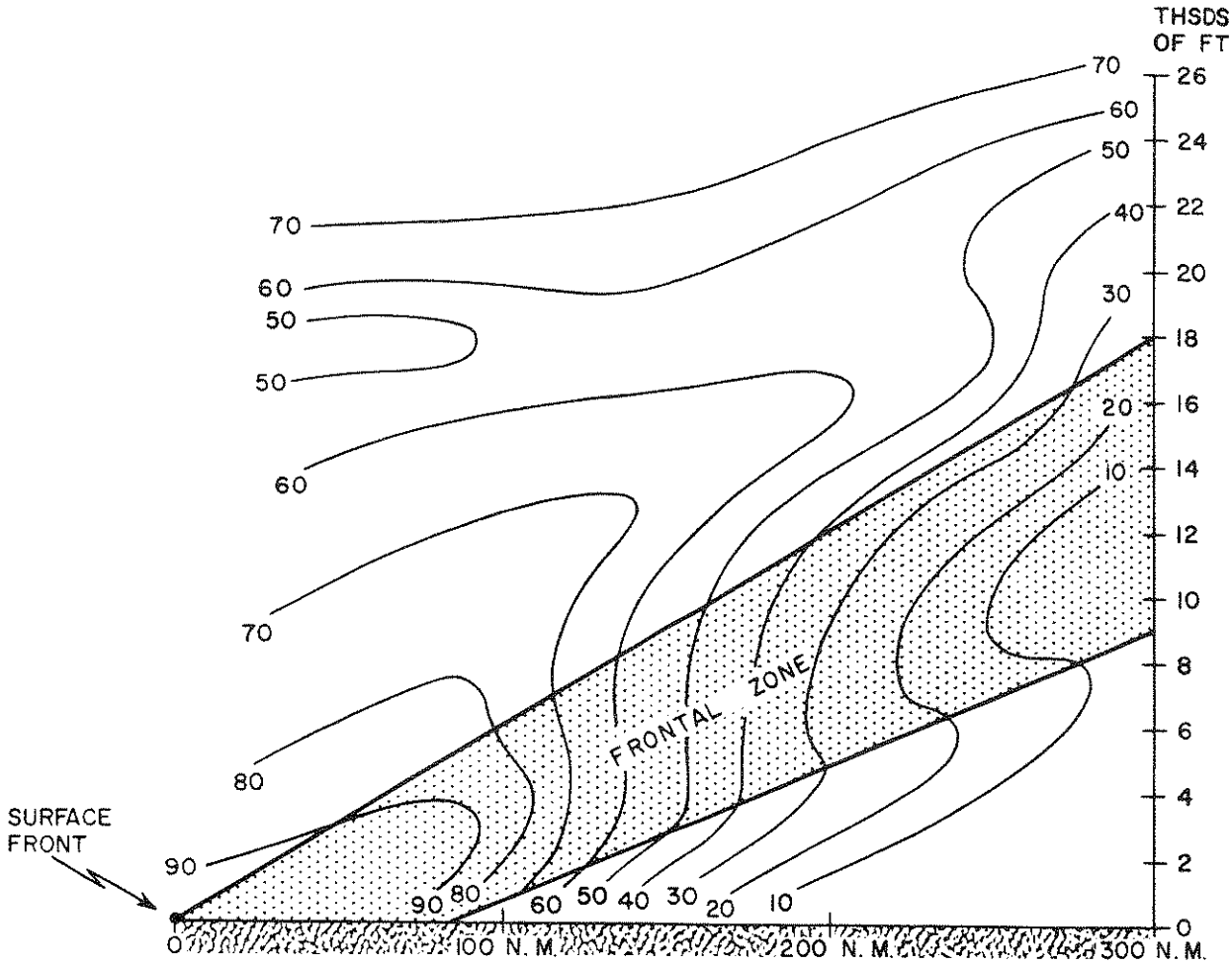

Figure 59. Frequency of Cloud Occurrence (in percent probability) in Active Warm Fronts Over Southern England (Sawyer and Dinsdale [57]).

warm fronts; it extended, on the average, down to 700 mb in cold fronts and 800 mb in warm fronts. In about half of the number of fronts, the driest air was found within the frontal zone itself; on occasions, it was found on both the cold and the warm sides of the zone. About half of the flights showed a sharp transition from moist to dry air, and the change in frost point on these flights averaged about 20°C in 35 miles. Some flights gave changes of more than 20°C in 20 miles.

As a frontal cloud deck is approached, the dew-point depression (or frost-point depression) starts diminishing rapidly in the close vicinity of the cloud (see Figure 60). Farther away than 10 to 15 miles from the cloud the variation was much less, and it was less systematic. This fact should be borne in mind when attempting to locate the edge of a cloud deck from raob humidity data (at 500 mb, for instance). Linear extrapolation or interpolation of dew-point depressions cannot be expected to yield good results. For instance, when one station shows a dew-point depression of 10°C and the neighboring station shows saturation, the frontal cloud may be anywhere between them, except within about 10 miles from the driest station. Figure 60 points out an advantage as well. Since frontal cloud masses at mid-tropospheric levels are usually surrounded by relatively dry air, *it is possible to locate the edge of the cloud mass from humidity data on constant-pressure charts, at least to within the distance between*

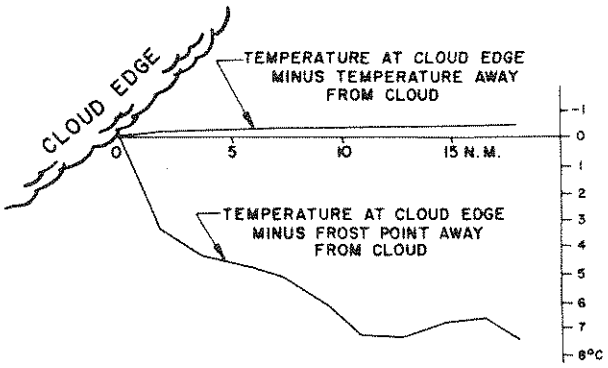

Figure 60. Average Horizontal Variation of Temperature and Frost Point in the Cloud-Free Air in the Vicinity of Frontal Cloud as a Function of the Distance from the Cloud Edge (Sawyer [56]).

neighboring soundings, even if the humidity data are not very accurate. This is so because the typical change of dew-point depression is going from the cloud edge to a distance of 10 to 15 miles or more into cloud-free air is considerably greater than the average error in the reported dew-point depression.

7.3. Temperature of the Cloud Top as a Condition for Type of Precipitation. The coalescence process may account for most of the precipitation which falls in the tropics and sub-tropics; the Bergeron-Findeisen theory, on the other hand, applies to most of the precipitation occurring in middle and high latitudes (in winter, at least). Whenever moderate or heavy rain falls in the temperature or arctic regions, it originates mainly in clouds that, in the upper portions at least, reach negative Celsius temperatures.

It has been found also that precipitating clouds usually extend for a considerable distance into sub-freezing temperatures. The difference in vapor pressure over ice and water reaches a maximum at -12°C. Mason and Howorth [40] found that over Northern Ireland, clouds less than 7500 feet thick with cloud-top temperatures warmer than -12°C and bases appreciably colder than 0°C rarely produced rain or snow.

Mason and Howorth [40] examined records from aircraft ascents through stratiform cloud over Northern Ireland (Aldergrove) and correlated these records with simultaneous hourly surface reports of precipitation. (The routine ascents rose to 400 mb.)

In the majority (87%) of cases when drizzle occurred, it fell from clouds whose cloud-top temperatures were warmer than -5°C, and which were, consequently, unlikely to contain ice crystals.

The frequency of rain or snow increased markedly when the cloud-top temperature fell below -12°C. When continuous rain or snow fell, the temperature in the coldest part of the cloud was below -12°C in 95% of the cases (41/43) and below -20°C in 84% of the cases (36/43).

Intermittent rain also was mostly associated with cold cloud tops, though cloud-top temperature above -12°C were somewhat more frequent with intermittent rain than with continuous rain. When intermittent rain was reported at the ground, the cloud-top temperature was below -12°C in 81% of the cases (46/57) and below -20°C in 63% of the cases (36/57). From this, it appears that *when rain or snow — continuous or intermittent — reaches the ground from stratiform clouds, the clouds, solid or layered, extend in most cases to heights where the temperature is below -12°C or even -20°C.*

This statement cannot, of course, be reversed. When no rain or snow is observed at the ground, middle cloud may well be present in regions where the temperature is below -12°C or -20°C. Whether precipitation reaches the ground or not will depend on the cloud thickness, the height of the cloud base, and on the dryness of the air below the base.

It is obvious that these findings may be of value in inferring the kind of precipitation to expect from forecasted cloud decks whose tops can be estimated as to height and temperature.

7.4. Inferring Clouds from Raobs. Theoretically, we should be able to infer from the radiosonde observations of temperature and humidity the layers where the sonde penetrated cloud layers. In practice, however, we find that the determinations we can make from the T and T_d curves are often less exact and less reliable than desired. Nevertheless, raobs give clues about cloud distribution and potential areas of cloud formation — clues which often cannot be obtained from any other source.

7.5.0. Systematic Errors in Radiosonde Humidity Elements. The great majority of humidity elements used in U.S. radiosondes are the carbon-impregnated plastic elements, ML-476/AMT. A limited number of sondes with the old lithium-chloride-coated plastic element ML-418/AMT-4 are still being used by the U.S. Navy and some foreign countries. The readings of this element tend to be too low.

7.5.1. Characteristics of the U.S. Lithium-Chloride Coated Humidity Element. Three characteristics of this humidity element combine to make the indicated relative humidity differ — at times appreciably — from the true (ambient) value.

a. The element has a variable time lag; i.e., a period of time must elapse before the element can adjust itself to the changing temperature and humidity in its surroundings. This adjustment is supposed to obey an exponential law, but the constants themselves in this exponential expression depend on the rate of change of both the temperature and the humidity. In practice, therefore, it is difficult to apply any corrections for this time lag except in a qualitative manner. It has been found experimentally that the time lag of this element can vary from 10 seconds to about 165 seconds. Also, the time lag, in general, increases with decreasing temperature [62]. The lag is largest when the element ascends from warm dry air into colder, moister air (this is usually the case when a radiosonde enters a more moist layer or a cloud). The radiosonde will then indicate dew points that are too low; if the temperature decrease continues upward through the cloud (as it usually does) the radiosonde may fail altogether to report dew-point depressions small enough for the existence of a cloud to be inferred. In this case, if the existing cloud is only a few thousand feet thick, either the indicated cloud base will be too high, or no cloud will be indicated. Conversely, if the radiosonde emerges from a cloud or a moist layer into a drier layer above, the time lag is smaller, being of the order of 10 to 20 seconds [17]. Thus, when using this element, the height of the top of a cloud layer or a moist layer is usually indicated more accurately than is the base of such layers.

b. When a humidity signal is transmitted by the radiosonde, a pulsating direct current flows through the element, causing it to polarize. This effect, which becomes more pronounced with time (i.e., during the ascent), results in an increase in the resistance of the humidity element and an indicated humidity that is too low.

c. At high humidities (such as those in clouds and precipitation), the lithium-chloride coating on the humidity element is sometimes washed out. This also results in reported humidities which are too low. The "washout" effect is particularly troublesome when one is attempting to locate the base and top of thick cloud layers. These clouds often produce precipitation (even though it may not reach the ground), and they usually have a layer of lower, wet clouds associated with them. Consequently, the humidity element has had its sensing power weakened before it enters the higher cloud layer.

The net effect of these three characteristics of the lithium-chloride coated humidity element is that the relative-humidity values reported are usually too low. These errors led to the development of the carbon-impregnated humidity element.

7.5.2 Characteristics of the Carbon-Impregnated Plastic Humidity Element. The ML-476/AMT humidity element is used in the AN/AMT-4( ), AN/AMT-12, and AN/AMQ-9 radiosondes, and in the AN/AMT-6

( ) and AN/AMT-13 radiosondes (dropsondes). The characteristics of this element are as follows:

a. The resistance of the element varies inversely with humidity changes of the atmosphere. The resistance ratio versus relative humidity characteristic of the ML-476/AMT is based on an absolute resistance at 33% relative humidity and a temperature of +25°C.

b. A limiting factor in making humidity measurements with this element is the fact that the time constant increases exponentially with decreasing temperatures; humidity values are unusable at temperatures colder than -40°C. The military specifications for the ML-476/AMT require that 63% of the total change in resistance of the element induced by a change in humidity from 20 ±5% to 90 ±5% shall occur in less than 2 seconds at +40°C and in less than 2 minutes at -40°C.

The accuracies of the ML-476/AMT are (as stated in the military specifications):

$T > 0°C, \pm 5\%$
$0°C \geq T \geq -40°C, \pm 10\%$
$T < -40°C$, questionable.

The above accuracies refer to one ascent from 15% to 90% humidity. An additional ± 4% for humidities > 33% and ± 5% for humidities < 33% should be allowed for relative humidities changing in the opposite direction (hysteresis) from 90% to 15%.

c. The range of defined accuracies of relative humidity values is 15% to 96%. The sensitivity is only fair at humidities less than about 15% and above 96%.

d. In comparison with the old lithium chloride element, the ML-476/AMT provides more accurate measurement of relative humidity, has less hysteresis effects, operates over a wider range of relative humidity and temperature, and responds more rapidly to changes in humidity.

7.5.3. Characteristics of Other Humidity Elements. The tests made several years ago at Payerne under WMO auspices indicated that most foreign radiosondes gave humidity readings which were acceptably compatible with those of the U.S. lithium-chloride element. Improvements in foreign humidity elements are being introduced which will tend to make them compatible with the carbon element at temperatures above freezing.

7.6. Dew Point and Frost Point in Clouds. The data-trace recorded from the humidity strip is calibrated in terms of the relative humidity with respect to water at negative, as well as positive, temperatures. The T_d value, the humidity parameter that is transmitted over the teletype, is the temperature to which the air must be cooled isobarically and at constant vapor pressure if saturation with respect to a water surface is to be reached. The *frost point* (i.e., the temperature to which the air has to be cooled or heated isobarically in order to reach saturation with respect to ice) is higher than the dew point, except at 0°C, where the two coincide. In the graph shown in Figure 61, the difference between dew point and frost point is plotted as a function of the dew point itself.

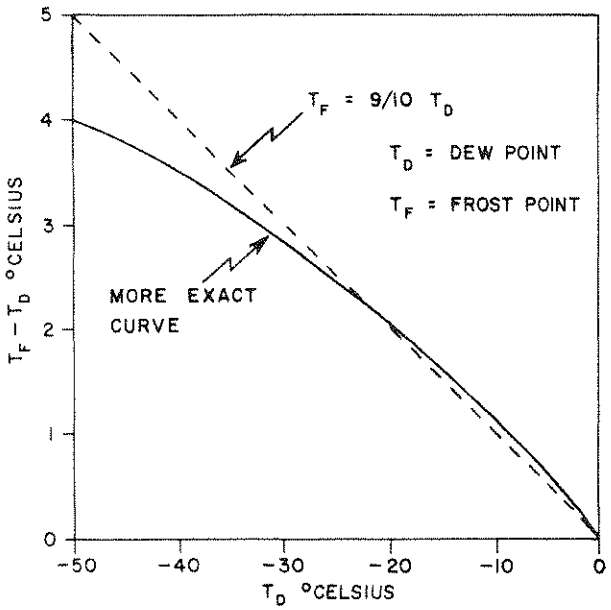

Figure 61. Difference Between Frost Point and Dew Point as a Function of the Dew Point.

In a cloud where the temperature is above freezing, the true dew point will coincide closely with the true temperature, indicating that the air between the cloud droplets is

practically saturated with respect to the water surface of the droplets. Minor discrepancies may occur when the cloud is not in an equilibrium state (e.g., when the cloud is dissolving or forming rapidly, or when precipitation is falling through the cloud with raindrops of slightly different temperatures than the air), but these discrepancies are theoretically small. In the subfreezing part of a cloud, the true temperature will be somewhere between the true dew point and the true frost point, depending on the ratio between the quantities of frozen and liquid cloud particles. If the cloud consists entirely of supercooled water droplets, the true temperature and the true dew point will, more or less, coincide. If the cloud consists entirely of ice, the temperature should coincide with the frost point. We cannot, therefore, look for the coincidence of dew points and temperatures as a criterion for clouds at subfreezing temperatures, even if the humidity element had no systematic errors of the nature discussed in paragraph 7.5.0. At temperatures below -12°C, the temperature is more likely to coincide with the frost point than with the dew point. The graph shown in Figure 61 indicates that the difference $(T_d - T_f)$ between the dew point and the frost point increases roughly 1°C for every 10°C that the dew point is below freezing; e.g., when T_d = -10°C, T_f = -9°C; when T_d = -20°C, T_f = -18°C; when T_d = -30°C, T_f = -27°C; etc. Thus, for a cirrus cloud that is in equilibrium (saturated with respect to ice) at a (frost-point) temperature of -40°C, the correct dew point would be -44°C (to the nearest whole degree).

We can state then, that in general, air in a cloud at temperatures below about -12°C is saturated with respect to ice, and that as the temperature of the cloud decreases (with height, e.g.), the true frost-point dew-point difference increases. The effects of these physical characteristics serve to reinforce the effects of the systematic faults of the humidity element itself (lag, polarization, and washout); i.e., they all conspire to make a radiosonde ascending through such a cloud indicate increasing dew-point depressions. Any attempt to determine the heights of cloud layers from the humidity data of a raob is, therefore, subject to errors from these effects. It is possible to overcome some of these errors by a subjective interpretation of the raobs, as discussed in the following paragraphs.

7.7. Examples of Interpretation of Raob with Respect to Cloud Layers, in Terms of Dew-Point Depression. Various Skew-T charts of soundings[27] made over the United States have been chosen to illustrate the behavior of the radiosonde during cloud penetration (see Figures 62a through 62j). During the time these soundings were being made, aircraft observations (from Project Cloud-Trail flights, *AWS TR 105-130* and *AWS TR 105-145)* of the heights of cloud bases and tops were made from aircraft flying in the vicinity of the ascending radiosondes. The difference — in time and space — between the aircraft and sounding observations was usually less than two hours and 30 miles. Some of the aircraft reported only the cloud observed above 15,000 feet; others reported all cloud. In Figures 62a through 62j, the aircraft cloud observations are entered in the bottom left corner of each diagram under the heading CLOUD; the surface weather report is entered under the aircraft cloud report. Where low cloud was not reported by the aircraft, the height of the cloud base may be obtained from the surface report. Aircraft height reports are in pressure-altitude. The temperature, frost-point, and dew-point curves are indicated by T, T_f, and T_d, respectively.

[27] All of the soundings illustrated and discussed here were made with U.S. radiosondes. Certain foreign equipment appears to have performance characteristics similar to those of the U.S. instruments; however, no soundings from foreign equipment have been examined in this study (see par. 7.5.0.).

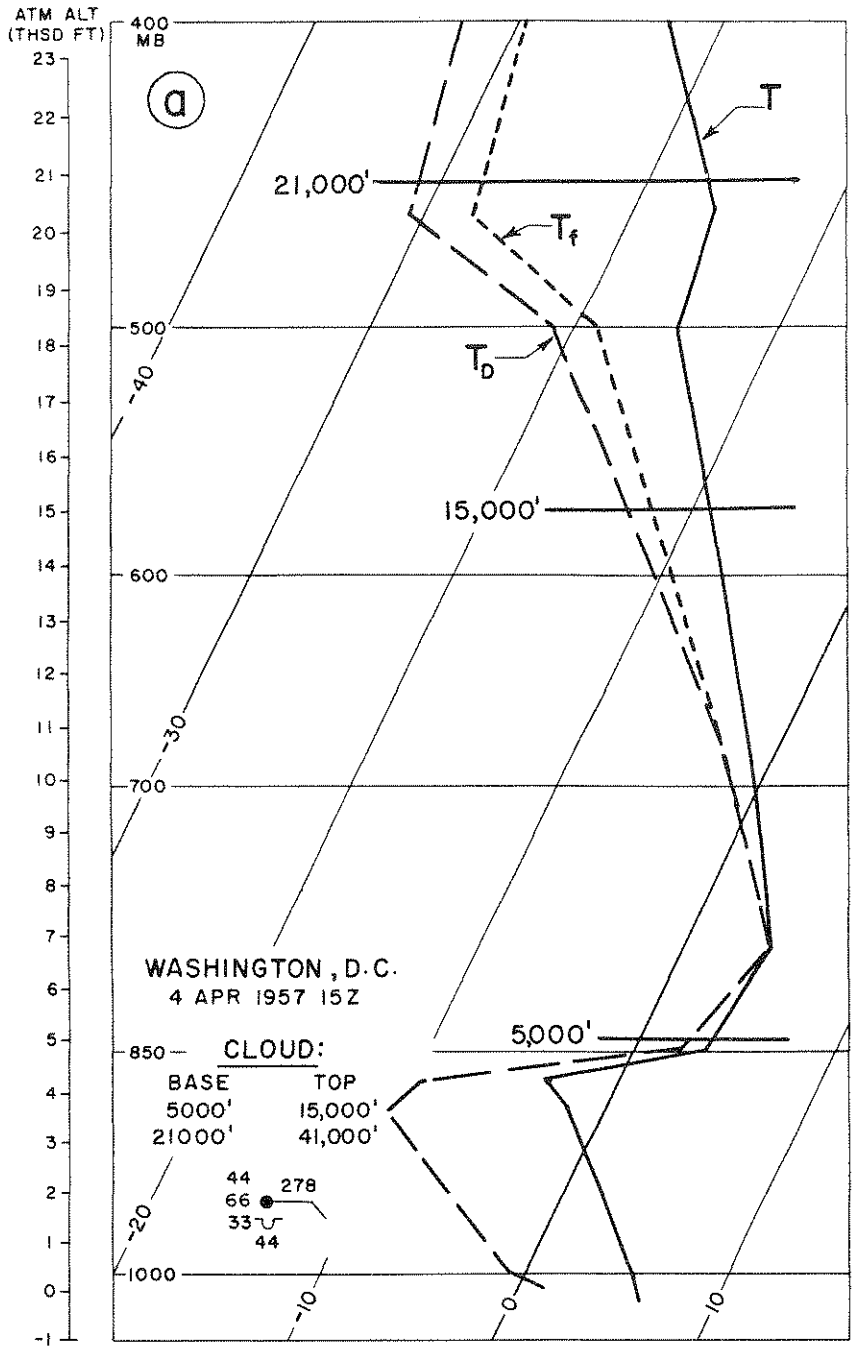

Figure 62a. Sounding in Marked Warm Front, Two Cloud Layers Indicated. A marked warm front is approaching from the south. Moderate, continuous rain fell two hours later. At 1830Z an aircraft reported solid cloud from 1000 to 44,000 feet (tropopause). The 15Z sounding shows an increasing dew-point depression with height, with no discontinuity at the reported cloud top at 15,000 feet. A definitely dry layer is indicated between 18,300 and 20,000 feet. The second reported cloud layer is indicated by a decrease in dew-point depression, but the humidity element obviously is slow in responding. The dew-point depression at the base of the cloud at 21,000 feet is 14°C and at 400 mb after about a 3-minute climb through cloud is still 10°C. From the sounding we should have inferred cloud from about 4500 feet (base of rapid humidity increase) to 500 mb and a second layer from 20,000 feet up. In view of the rapid filling of the cloud-free gap between 15,000 and 21,000 feet which followed as the warm front approached, the agreement between reported and inferred conditions is good.

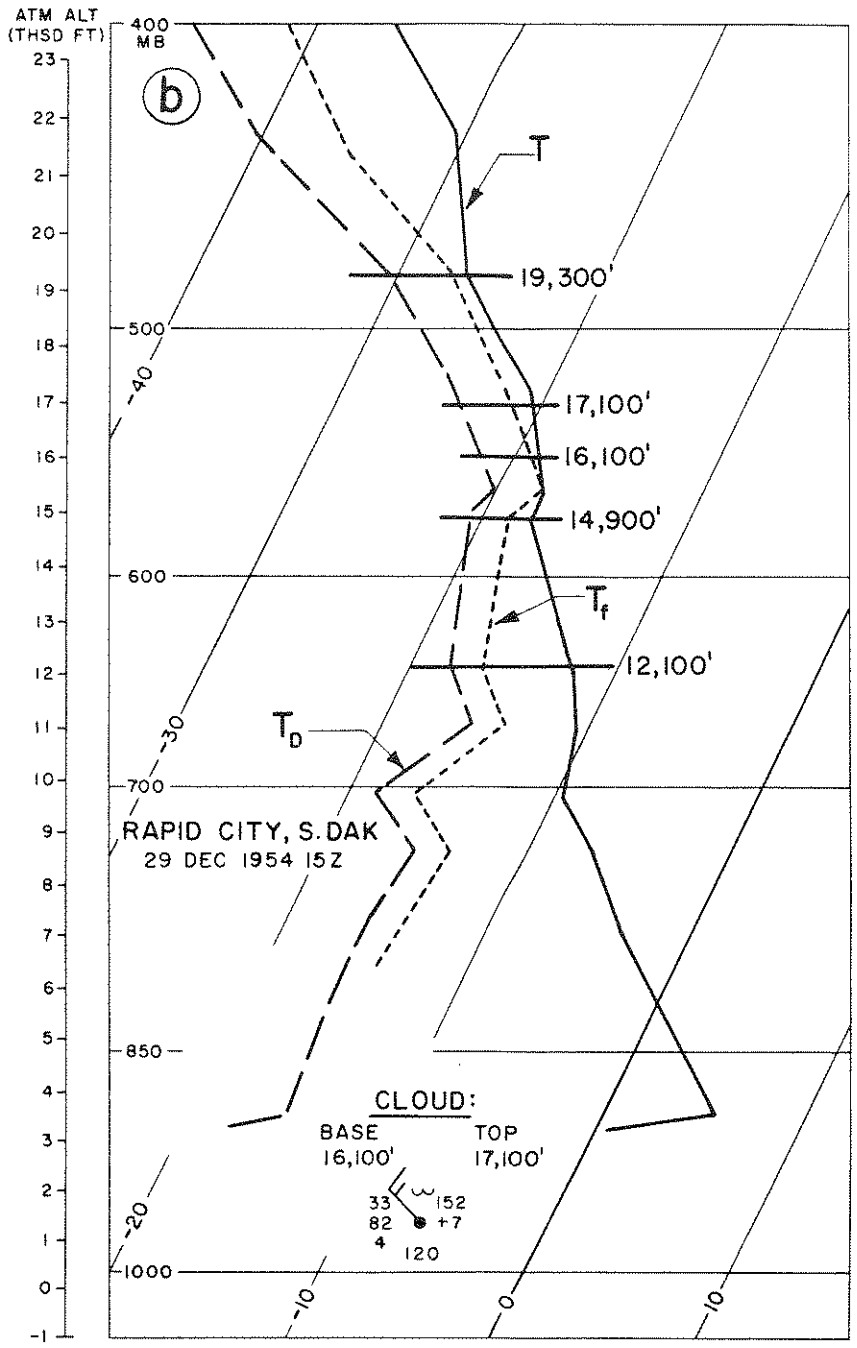

Figure 62b. Cold Front with Cloud Layer Thinner Than Indicated by Sounding. A cold front lay E-W across North Dakota at 15Z. The reported cloud layer was much thinner than would be inferred from the sounding. Using the rule that a cloud base is indicated by a fairly rapid decrease in dew-point depression to a dew-point depression of 6°C or less, we should put the base somewhere between 12,100 and 14,900 feet. Similarly, we should have expected the cloud to extend to 19,300 feet where the dew-point depression starts increasing again. The surface report places the base at 12,000 feet. It is possible that the difference in space and time between the aircraft and the sonde may account for the discrepancy. Of the two possibilities, 12,100 and 14,900 feet, we should choose the latter as base height. If a decrease in dew-point depression is followed by a much stronger decrease, choose the height of the base of the stronger decrease as the cloud-base height.

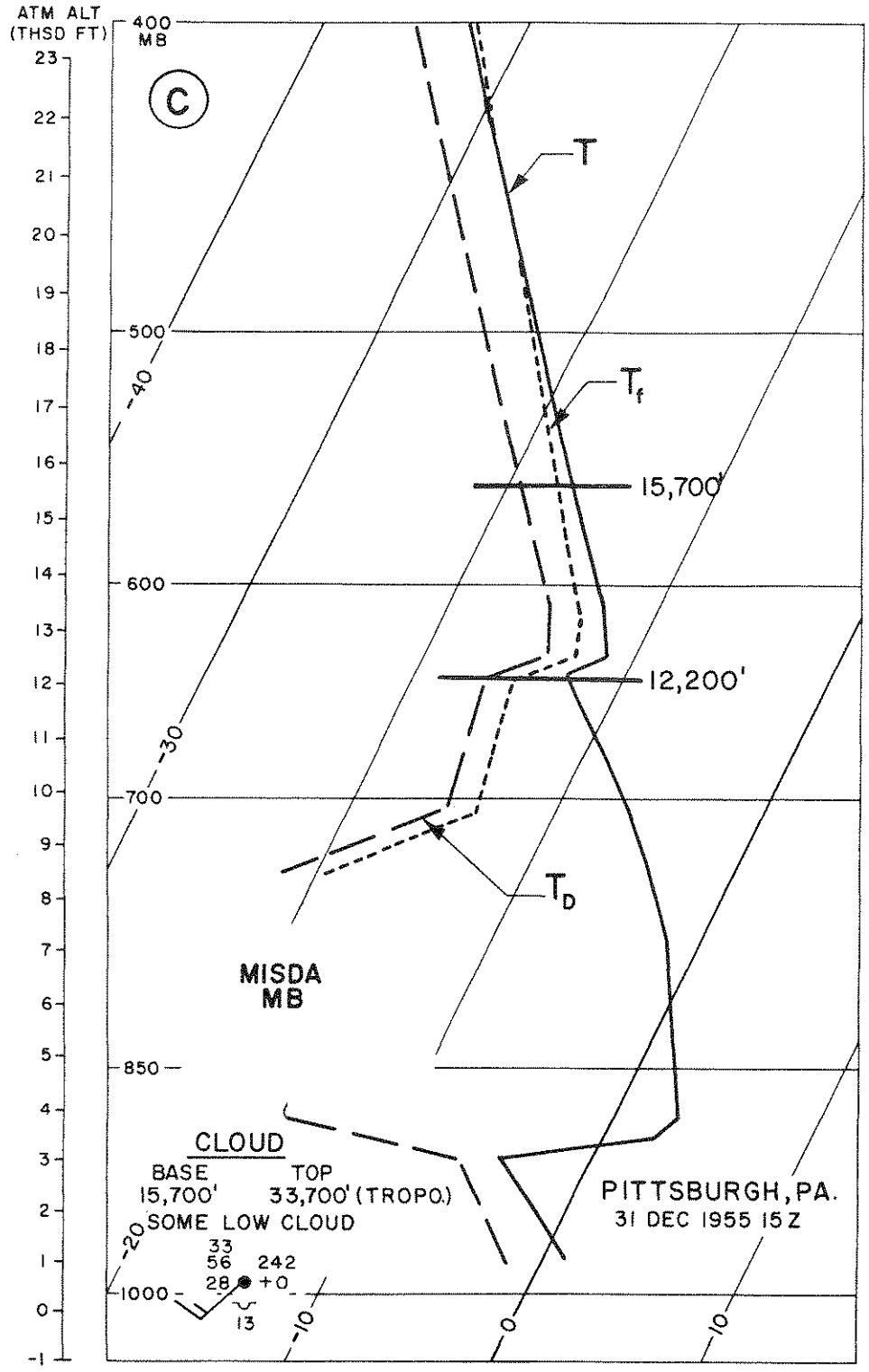

Figure 62c. Middle-Cloud Layer with No Precipitation Reaching the Surface. This is a case of cloud in the 500-mb surface with no precipitation reaching the surface; the nearest rain at the time was in Tennessee. The evidence from the sounding for putting the cloud base at 12,200 feet is strong, yet the base is inexplicably reported at 15,700 feet. The reported cloud base of 15,700 was probably not representative, since altostratus, with bases 11,000 to 14,000 feet, was reported at most stations over Ohio and West Virginia.

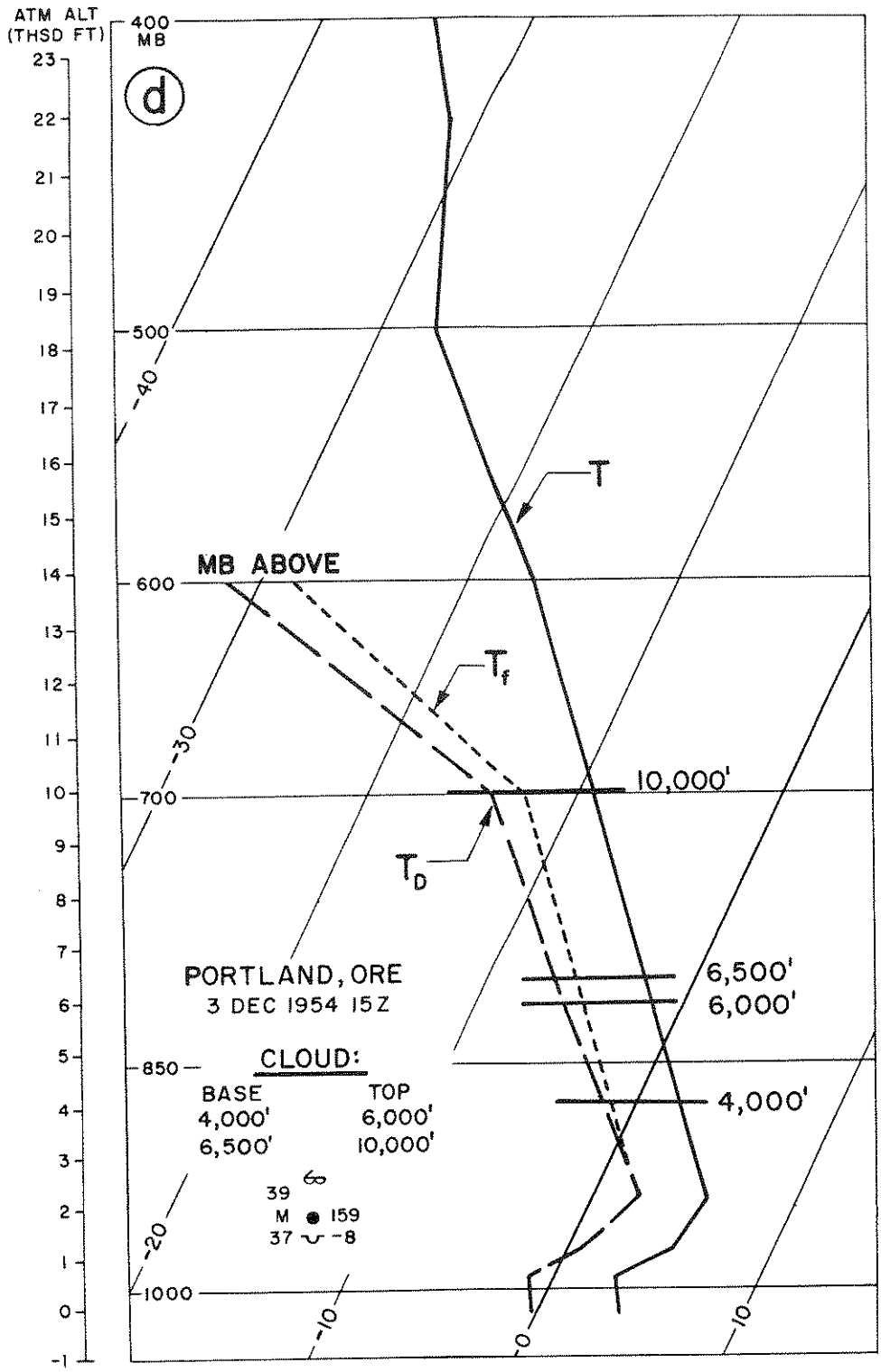

Figure 62d. Layer Clouds with Their Intermediate Clear Layers not Showing in Humidity Trace. There is good agreement between the sounding and the aircraft report. The clear layer between 6000 and 6500 feet is not indicated on the sounding. Thin clear layers as well as thin cloud layers usually cannot be recognized on the humidity trace.

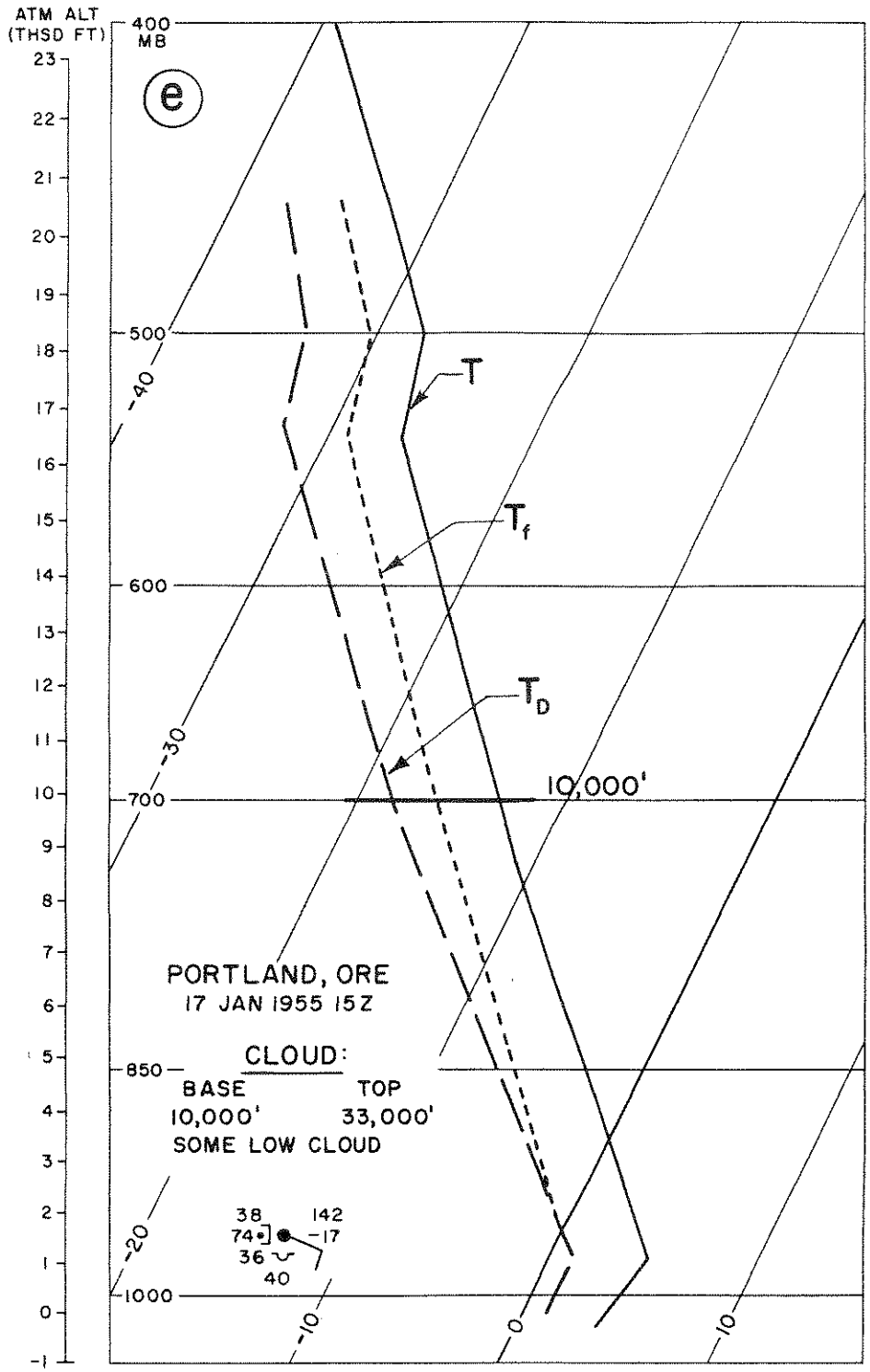

Figure 62e. Deep Layer of Cloud from Lower Levels to Tropopause with Some Clear Layers not Revealed by Sounding. There is cloud from 4000 feet to the tropopause, with the exception of an unspecified clear layer between the top of the low stratocumulus and the base of the middle cloud at 10,000 feet. From the sounding, there is little indication of any layering, and the dew-point depression is 4°C to 6°C throughout the sounding. This sounding is typical of solid or near-solid cloud from the surface to great heights in moderately cold atmosphere (500-mb temperature about -30°C).

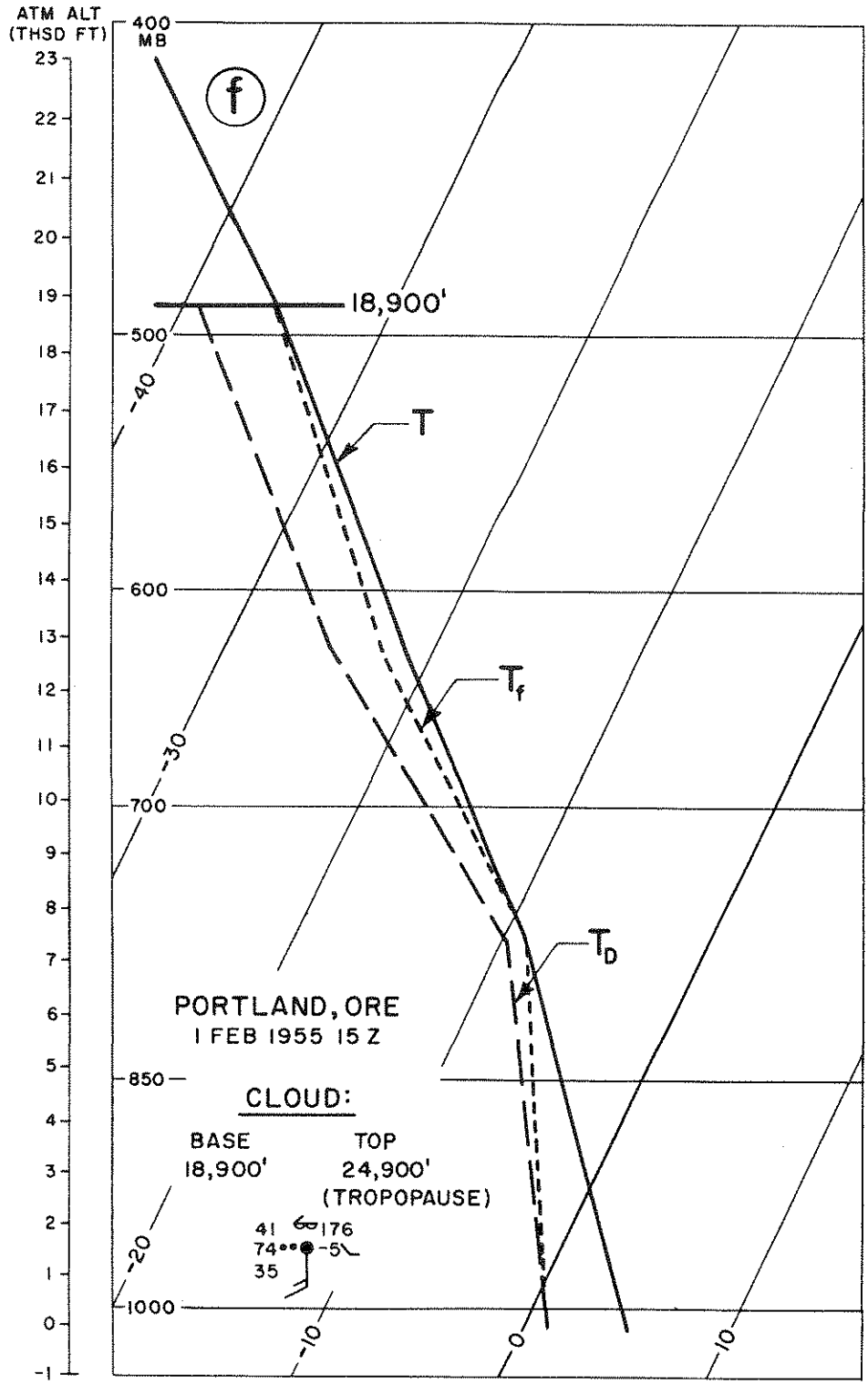

Figure 62f. This Sounding is Similar to that Shown in Figure 62e. From this sounding we should have inferred solid cloud from near ground to above 500 mb. An occlusion was 30 miles west of Portland and was associated with a widespread rain area. The discrepancy between sounding indications and observed cloud is hard to explain.

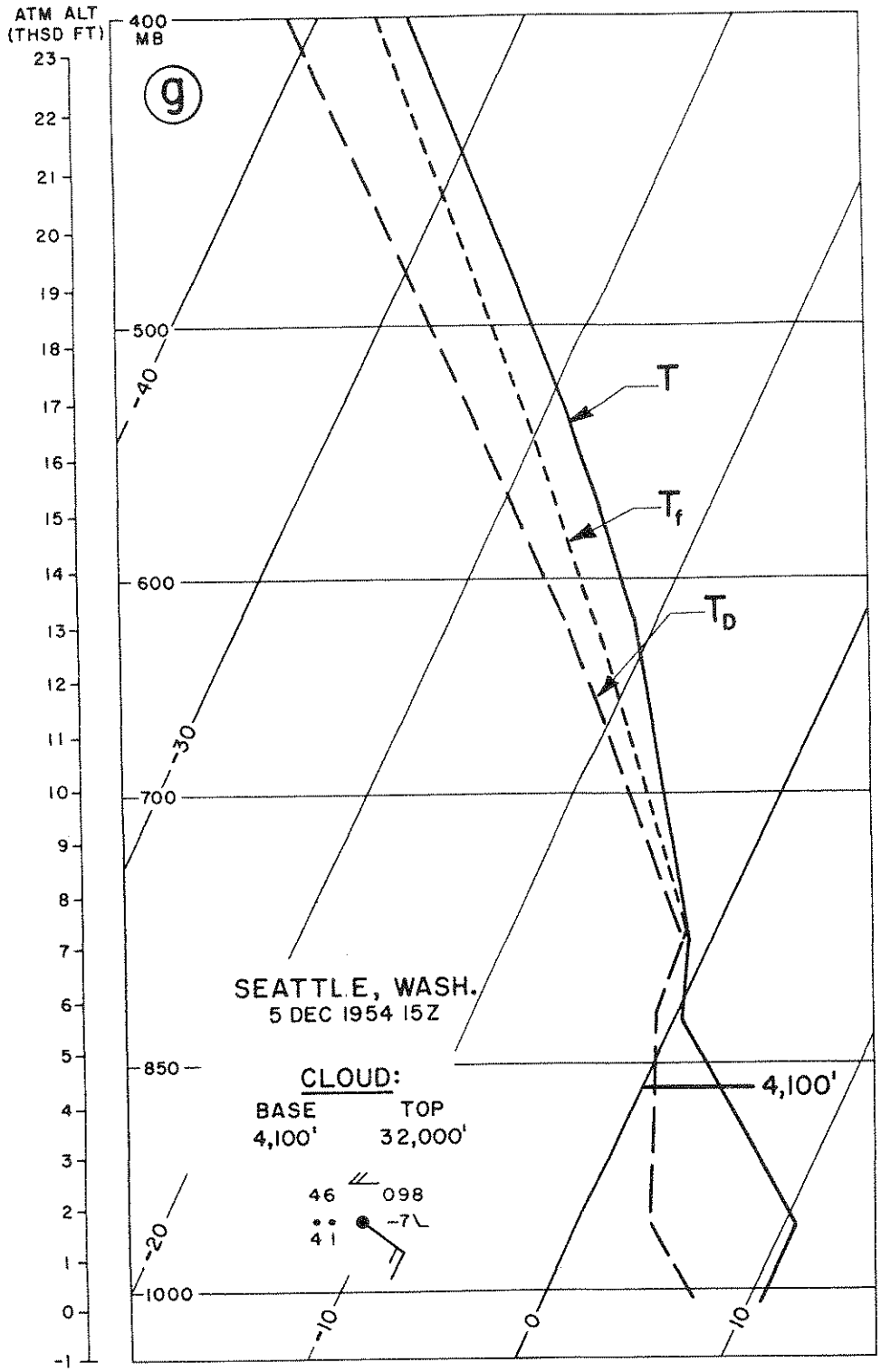

Figure 62g. Deep Cloud Layer, Sounding Showing Base Too High. There is good agreement between sounding indications and the observed cloud except for the cloud base, for which the sounding indicates the height to be at 5500 feet. (If a decrease in dew-point depression is followed by a much stronger decrease, choose the height of the base of the stronger decrease as the cloud-base height.)

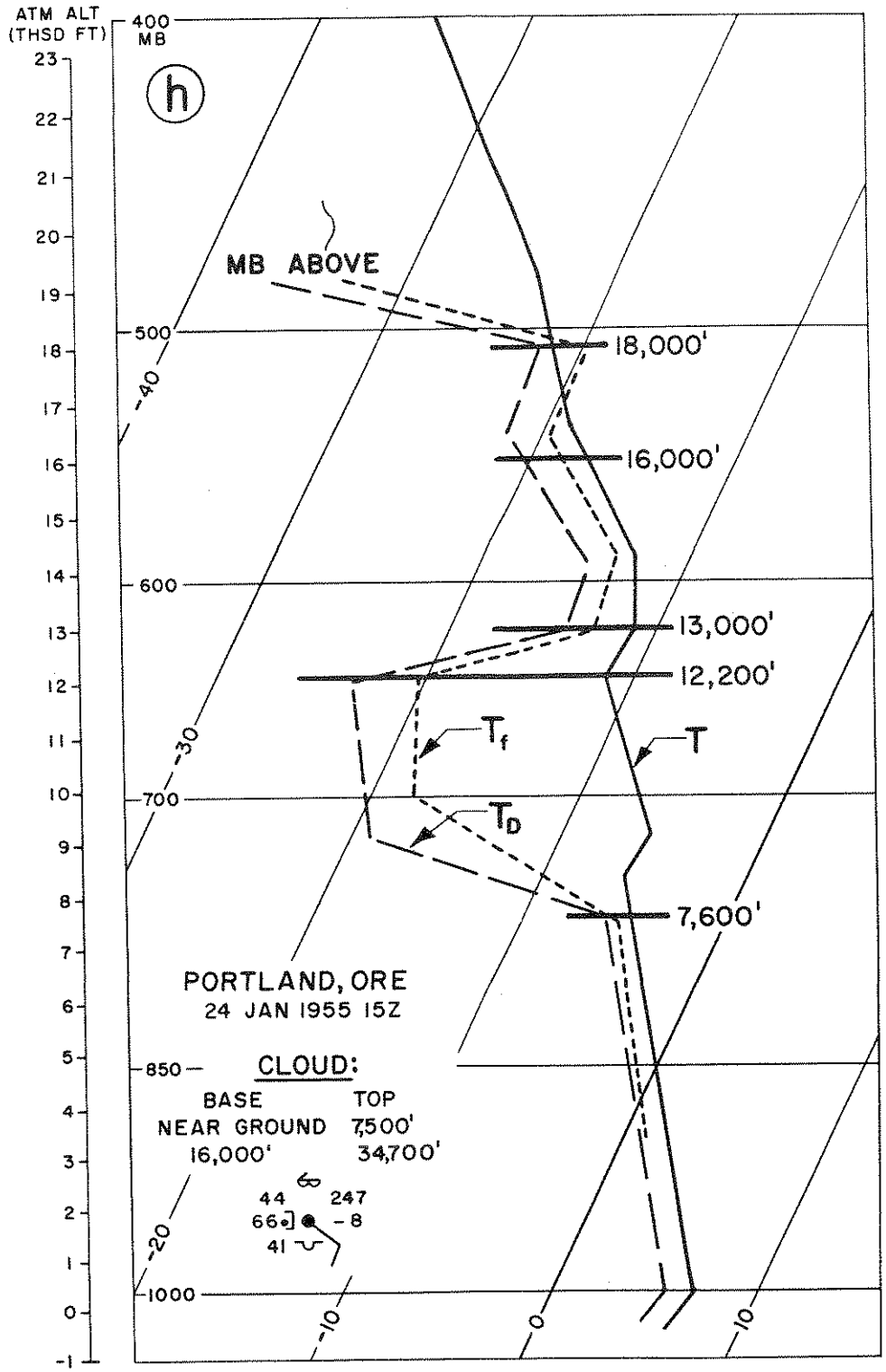

Figure 62h. Double Layer of Cloud, Top of Upper Layer not Indicated by Sounding. A cold front was located 200 miles west of Portland. There is good agreement between observed and sounding-indicated cloud heights of the first layer. The sounding indicates a second layer based at 12,200 feet and definitely terminating at 18,000 feet. The aircraft reported solid cloud from 16,000 feet to near the tropopause. The most likely explanation: something went wrong with the humidity element above 18,000 feet.

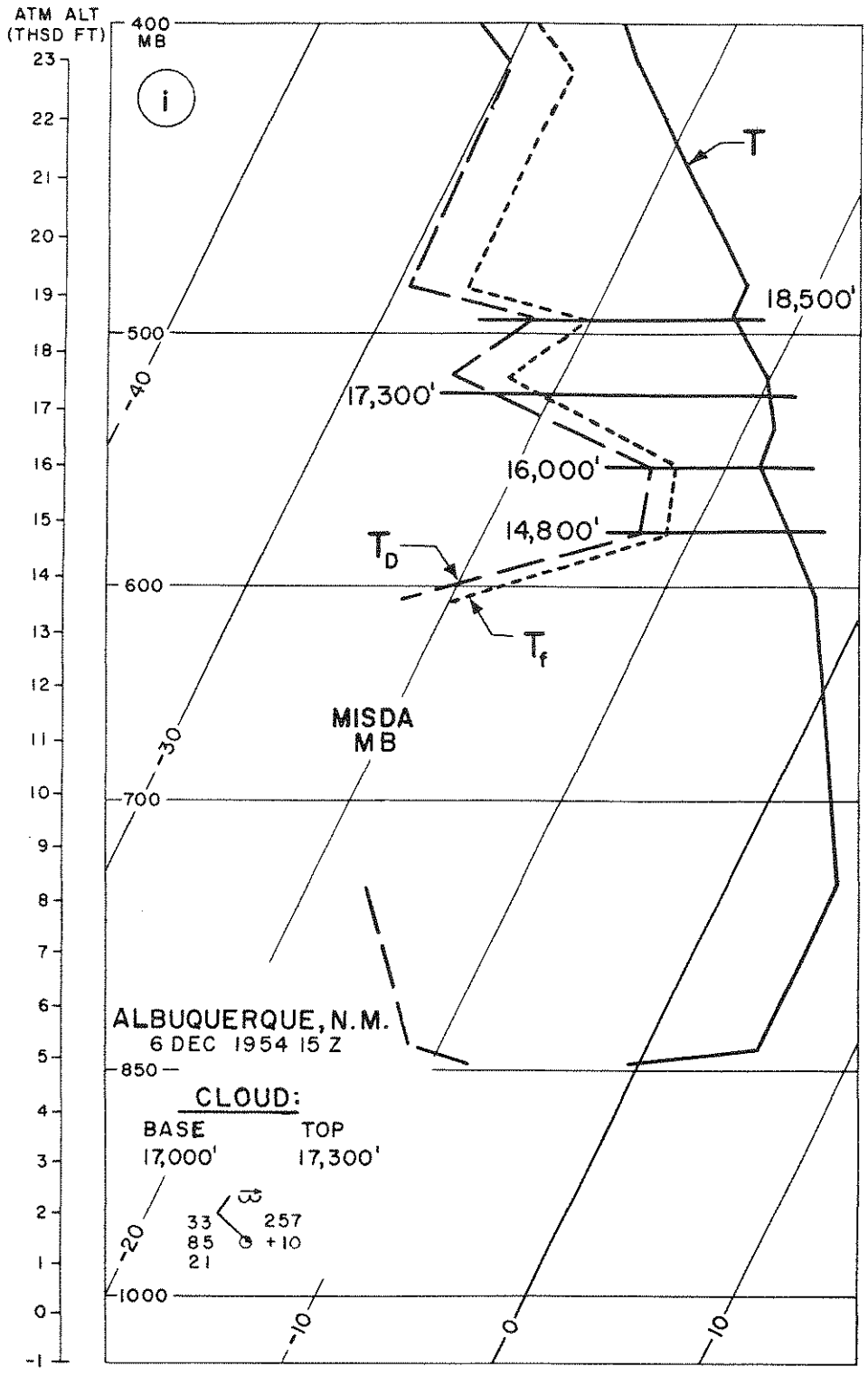

Figure 62i. Sounding Through Scattered Thin-Layered Middle Clouds Indicated by Variable Humidity. The sounding indicates considerable variability in the humidity trace. If any cloud could be inferred, it would be from 14,800 to 16,000 feet and at 18,500 feet. The height of the thin scattered layer observed at 17,000 feet is not well fixed by the sounding. This sounding is typical of thin layered middle clouds, usually scattered or broken.

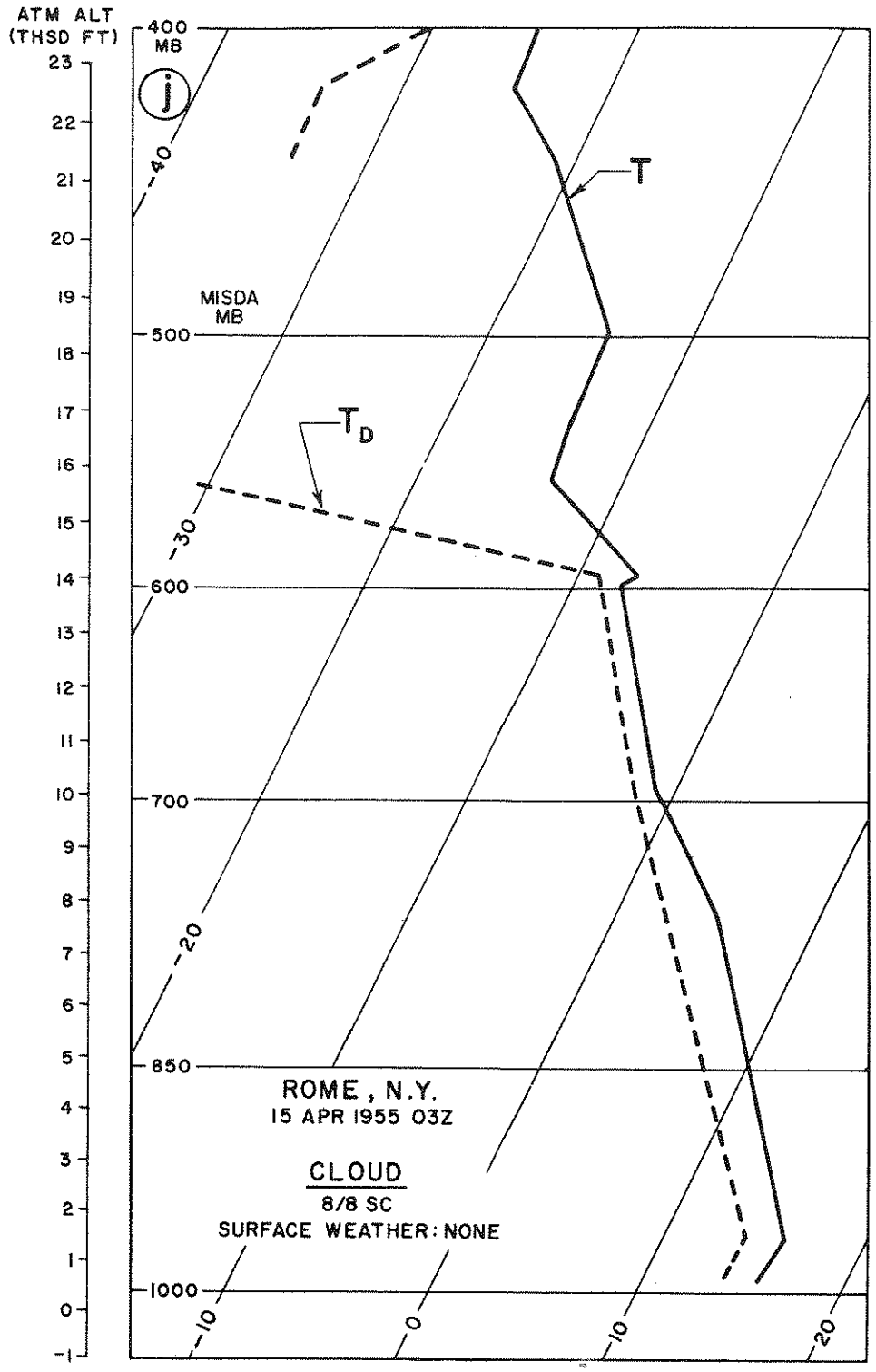

Figure 62j. Sounding Showing a Spurious Superadiabatic Lapse Rate where Sonde Leaves Top of Cloud. No aircraft reports were available. The sounding illustrates that the lapse rate is, at times, recorded as superadiabatic when the sonde leaves a cloud top and enters extremely dry air above the cloud. The phenomenon has been ascribed to a wet-bulb effect on the thermistor (see par. 5.6).

Comparisons of the type made above between soundings and cloud reports from aircraft provide us with the following rules:

a. A cloud base is almost always found in a layer (indicated by the sounding) where the dew-point depression decreases.

b. The dew-point depression usually decreases to between 0°C and 6°C when a cloud is associated with the decrease. In other words, we should not always associate a cloud with a layer of dew-point decrease but only when the decrease leads to a minimum dew-point depression $< 6°C$; at cold temperatures (below -25°C), however, dew-point depressions in cloud are reported as $> 6°C$.

c. The dew-point depression in a cloud is, on the average, smaller for higher temperatures. Typical dew-point depressions are 1°C to 2°C at temperatures of 0°C and above, and 4°C between -10°C and -20°C.

d. The base of a cloud should be located at the base of the layer of decreasing dew-point depression, if the decrease is sharp.

e. If a layer of decrease of dew-point depression is followed by a layer of stronger decrease, the cloud base should be identified with the base of the layer of strongest decrease.

f. The top of a cloud layer is usually indicated by an increase in dew-point depression. Once a cloud base is determined, the cloud is assumed to extend up to a level where a significant increase in dew-point depression starts. The gradual increase of dew-point depression with height that occurs on the average in a cloud is not significant.

In addition to the above analysis of Project Cloud-Trail data, another study was made in Hq AWS to see how reliable the dew-point depression is as an indicator of clouds. Raobs for January 1953 from 29 U.S. Weather Bureau stations were compared with cloud-base observations taken at the same location and approximate time of each raob. The results of this study are summarized in the two graphs shown in Figure 63. (A more complete discussion of this study is given in Attachment 1 to this manual.) Each graph shows the percent probability of the existence of a cloud layer in January for different values of the dew-point depression. On each graph one curve shows the probability of clear or scattered conditions as a function of the dew-point depression; the other curve, that of broken or overcast conditions. Separate graphs are included for the 1000- to 850-mb and 850- to 600-mb layers. The graphs are based on 1027 observations, which are enough to indicate the order of magnitude of the dew-point depressions at the base of winter cloud layers. (The small irregularities in the curves were not "smoothed out" because

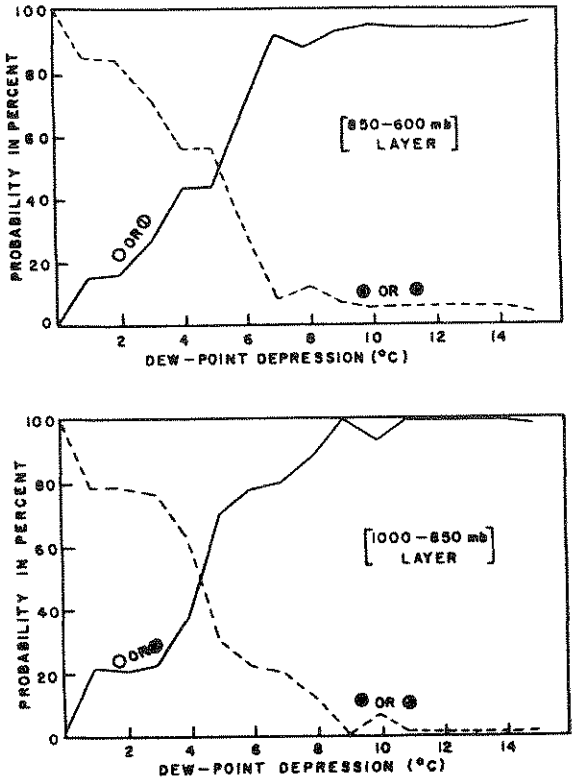

Figure 63. Percent Probability of the Existence of Cloud-Layer Bases for Different Values of Dew-Point Depression (°C). Solid lines represent probability of clear or scattered conditions; dashed lines, the probability of broken or overcast conditions with the cloud-layer bases between 1000 mb and 600 mb.

it is not certain that they are all due to insufficient data.) The graphs are applicable without reference to the synoptic situation. For a given winter sounding, one can estimate from the graph the probability of different sky-cover conditions with cloud bases between 1000 mb and 600 mb for layers of given minimum dew-point depressions.

7.8. Motorboating and Missing Data. "Motorboating" is a term used to describe the radiosonde's signal when the humidity is below the perceptible level of the element. A distinction must be made on the Skew-T

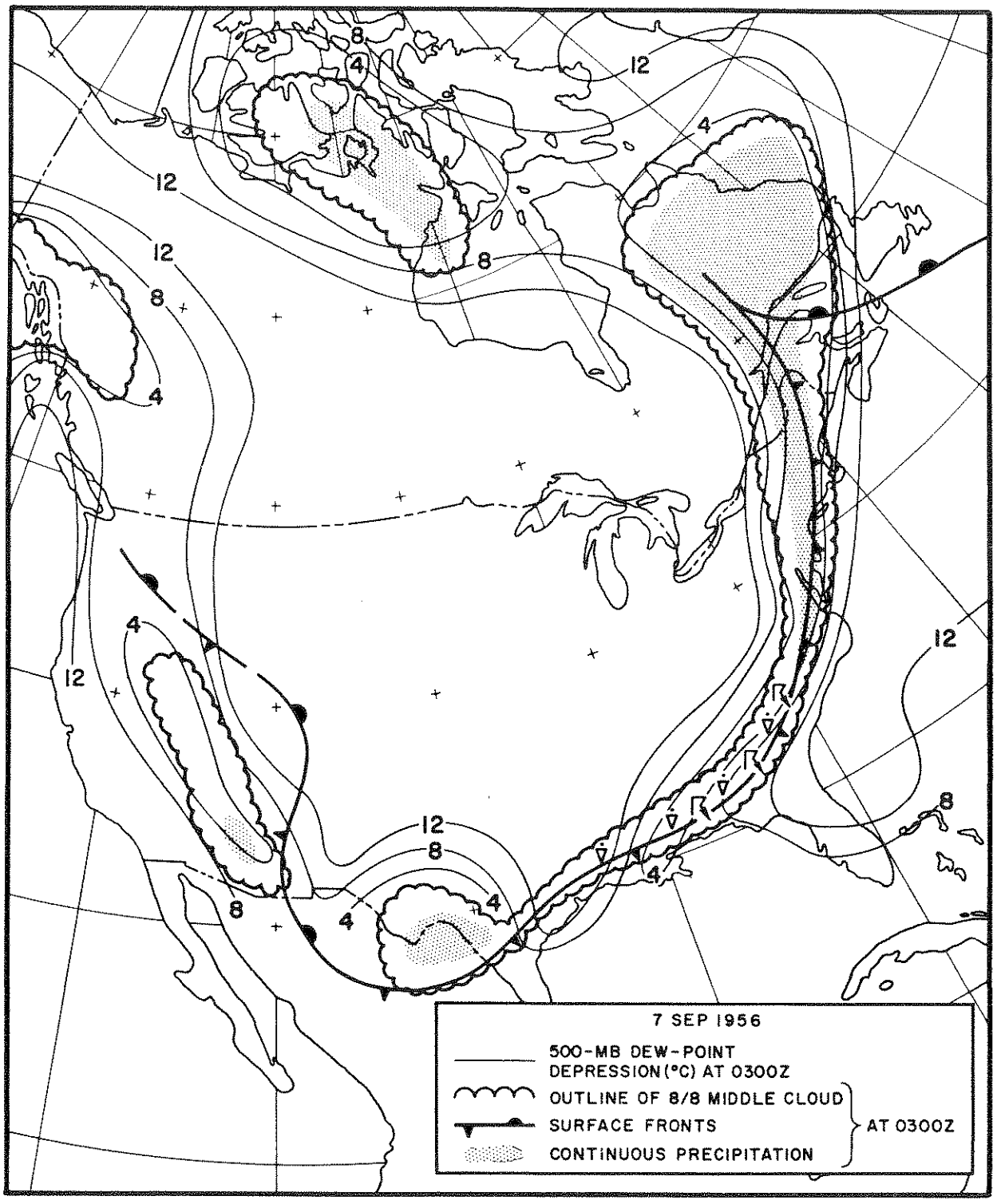

Figure 64. Surface Fronts, Areas of Continuous Precipitation, Areas Covered by 8/8 Middle Clouds, and Isolines of 500-mb Dew-Point Depression at 03Z, 7 September 1956.

plot between "motorboating" and "missing data." This distinction is often neglected. "Motorboating" should always be indicated as MB; "missing data" as MISDA (see par. 3.4). The confusion occurs because both cases are coded as a dew point of XX.

If the dew point is missing for reasons other than "motorboating," the case can be recognized by the additional data-group 10168 at the end of the transmission: The group 10168 is followed by one or more groups $OP_1P_1P_2P_2$, where P_1P_1 and P_2P_2 are the lower and upper levels of the stratum of missing data in tens of millibars.

When the temperature is below -40°C, no humidity data are sent; the humidity element is considered too unreliable at these low temperatures (see FMH No. 3, *Radiosonde Observations*, latest edition, as amended).

7.9. 500-mb Analysis of Dew-Point Depression. Figure 64 shows an analysis of the 500-mb dew-point-depression field, superimposed upon an analysis (based upon the surface observations) of areas of continuous precipitation and of areas of overcast middle cloud. The 500-mb dew-point-depression isopleths were drawn independently of the surface data. The analyses show that:

a. The regions of high humidity at 500 mb coincide well with the areas of middle cloud and the areas of precipitation.

b. The regions of high humidity at 500 mb are separated from the extensive dry regions by strong humidity gradients. These gradients are, in all probability, much stronger than shown on this analysis, since this analysis has the defect of all continuous-field analyses which are based on discrete observations spaced widely apart; i.e., linear interpolation between observations smoothes out strong contrasts.

c. A dew-point depression of 4°C or less is characteristic of the larger part of the areas of continuous precipitation and also of the larger part of the areas of overcast middle clouds.

Since the 500-mb dew-point-depression analysis agrees well with the surface analysis of middle cloud and precipitation, the possibility exists of replacing or supplementing one of these analyses with the other.

The characteristics (outlined above) of the 500-mb dew-point-depression analysis make it a valuable adjunct to the surface analysis. These analyses can be compared; and, by cross-checking, each can be completed with greater accuracy than if it were done independently.

A rough sketch of the dew-point-depression field may be completed on the facsimile chart in an few minutes. The dew-point depressions are now plotted on the upper-air analyses. Station circles are filled in where the depression is 5°C or less, which facilitates a quick appraisal of the dew-point-depression field.

7.10. Three-Dimensional Humidity Analysis — The Moist Layer. A single-level (e.g., 500-mb) dew-point-depression analysis to find probable cloud areas does not indicate clouds above or below that level. For example, if the top of a cloud system reached only to 16,000 feet, and there were dry air above at 500 mb, we would never suspect, from the 500-mb analysis, the existence of cloud a short distance below the 500-mb level. (Admittedly, this is a hypothetical case; under such conditions, the raob would probably show humid conditions at 500 mb as well, even though the cloud top was actually below 500 mb.)

However, an analysis of the extension of the moist layers in three dimensions can be obtained simply by scrutinizing each individual raob. The raobs selected should be those for the general vicinity of, and the area 500 to 1200 miles upstream of, the area of interest, depending on the forecast period. (Most systems during a 36-hour period will move less than 1200 miles.) The moist layers, apart from the surface layers, can be determined by the methods described in paragraph 7.7. The heights of the bases and tops (labeled in thousands of feet of pressure altitude) are plotted at the raob-station location on the 500-mb chart. If more than one layer is present, this fact can be indicated, though there is little advantage in indicating a dry

layer 2000 to 3000 feet (or less) thick sandwiched between thicker moist layers. Usually, it is sufficient to indicate the entire moist layer, without bothering about any finer structure. A survey of the field is made easier by writing the heights of the bases in one color and the heights of the tops in another. It is not recommended that isopleths be drawn for the height of the bases and the tops, because the moist layer is not a well-defined entity.

If more specific and objective directions than those given in paragraph 7.7 are desired (as would be the case when non-professional persons are to select the moist layer), a moist layer may be defined as a layer having a frost-point depression of 3°C or less (i.e., a dew-point depression of 4°C at -10°C; 5°C at -20°C; 6°C at -30°C; etc.)

7.11. Limitations to Diagnosis of Tall Cumulus and Cumulonimbus Distribution from Raobs. The cumulus and cumulonimbus of summer and tropical air-mass situations are generally scattered and in many, if not most cases, they do not actually cover over half of the sky. Under such conditions the probability of a radiosonde, released once to four times daily at a fixed time and place, passing up through a cloud of this type, appears to be small. When a balloon does enter the base of a tall cumulus cloud it is likely to pass out of the side of the cloud rather than the top, or it may get caught for a time in a downdraft, giving an ambiguous record of the vertical-cloud distribution.

For the above reasons, experience indicates that little dependence can be placed on the usual soundings to indicate directly the existence of tall cumulus in the area. On the other hand, where the radiosonde samples the environment of such clouds, a stability analysis combined with consideration of surface-weather observations, radar and aircraft reports, and synoptic analysis for heating and convergence, will usually provide an estimate of the extent of cumulus sky coverage. This approach uses the same principles and procedures as in thunderstorm and severe-convective weather forecasting, which are referenced in chapter 8 of this manual.

In those cases where the sounding passes up through a cumulus, it is well to keep in mind that the temperature in parts of such clouds is often colder than the environment just outside the cloud — especially due to "overshooting" or hail in regions of very strong updraft. These colder regions may still have buoyancy relative to other parts of the cloud surrounding them. Also, old dissipating cumulonimbus clouds are generally slightly colder than their environment.

The lapse rate in cumulus and cumulonimbus is not necessarily saturation adiabatic, owing to effects of "holes," downdrafts, melting of snow or hail, entrainment, mixing, etc.

Soundings made vertically through cumuliform clouds by means of aircraft or sailplanes are more indicative of their real structure than raobs; examples from various special projects are numerous in the literature (see, for example, [18] [37] [38] [45]).

7.12. Indications of Cirrus Clouds in Raobs. True cirrus forms at temperatures near -40°C or colder and consists of ice crystals. At these temperatures as soon as the air is brought to saturation over water the condensate immediately freezes. The crystals then often descend slowly to levels of -30°C, and persist for a long time if the humidity below the formation level is high enough. In general, cirrus is found in layers which have saturation or supersaturation with respect to ice (at any temperature colder than 0°C, if the RH with respect to water is 100%, then the RH with respect to ice is >100%). Observations from special aircraft soundings with frost-point or dew-point hygrometers, indicated that the layers where cirrus occur are not always saturated with respect to ice and often occur with as much as 3°F frost-point depression; but this may be in part due to error in the instruments. When the aircraft noted "cirrus in the distance" at its height, a relative moist layer (frost-point depressions less than 15°F or 20°F) was usually being passed through [43] .

Present radiosonde humidity elements are far from capable of measuring humidity *values* satisfactorily at the temperatures of the cirrus levels. However, the elements will often show *change* in humidity at low temperatures that reflect the presence of the moist layers which contain cirrus. If the transmitted sounding data would include the heights at which the humidity trace at high levels indicates an increase, or the maximum height to which any humidity is shown, useful inferences of probability of cirrus could be made therefrom. This was suggested by an examination of some humidity traces on radiosonde records taken in conjunction with Project Cloud-Trail (*AWS TR 105-130* and *AWS TR 105-145*).

Several studies have pointed to indirect indications of cirrus presence whenever the dew-point depression at 500, 540, and 400 mb was relatively low [34] . Bannon [9] [10] found a correlation of 0.80 between temperature at 500 mb and frost point at 300 mb and 0.82 between $T_{(500)}$ and $T_{f(250)}$.

Results of efforts to find a relation between changes in lapse rate and the occurrence of cirrus have not been very convincing and it is doubtful on *a priori* grounds that any such simple universal relation should be expected (*AWS TR 105-130*).

Appleman has shown how his contrail-forecasting curves (when overlaid on the Skew-T Chart) can be used to improve the accuracy of ground-observer estimates of the height of *observed* cirrus layers (see *AWS TR 105-110* and *AWS TR 105-110A* for details of procedure and tests).

Chapter 8

FORECASTING USES OF RAOBS PLOTTED ON ADIABATIC CHARTS

8.1. General. Increasing dependence of detachments on centrally-produced analyses and prognoses has reduced the role of raob analysis. AWS philosophy on the use of the computer products and guidance on the use of raobs in conjunction with facsimile charts is outlined in AWSM 105-55 (rescinded, but can be used for background information). Some special techniques that require evaluations from analyzed and/or forecast soundings were developed by AWS for: severe convective storms, aircraft icing, contrails, anomalous propagation and refractive index, fog, and density altitude. Techniques for forecasting other phenomena from soundings, such as maximum temperatures and clouds, have been described in the literature.

8.2. Severe Convective Storms. The AWS Military Weather Warning Center (MWWC) employs specialized raob analysis techniques to identify airmass types favorable for severe weather, to evaluate various derived indexes of stability, to construct forecast soundings, and to semi-objectively evaluate hail size and maximum wind-gusts. Most of the MWWC routines are too sophisticated and time consuming for ordinary detachment use. The evaluation of many of these indexes has been computerized. However, several of the MWWC procedures that are described in AWS Technical Report 200 can be used in the detachment. A number of objective local-forecast studies for prediction of thunderstorms that use predictors taken from the sounding are listed in AWS TR 105-19 and AWSP 0-13.

8.3. Aircraft Icing. AWS Manual 105-39 describes procedures developed by AWS for forecasting icing. One procedure, which uses an overlay to the Skew-T diagram as an aid for determining the probable type and intensity of icing from a current or forecast sounding, has been computerized at the Air Force Global Weather Central (AFGWC).

8.4. Contrails. The AWS procedure for forecasting contrails is described in AWS Manual 105-100. This technique, which employs either curves overprinted on the Skew-T chart (DOD WPC-9-16) or a transparent overlay for this chart, has been computerized at AFGWC.

8.5. Anomalous Propagation and Refractive Index. The estimation of radio and radar refraction due to the atmosphere is treated comprehensively in AWS TR 184 (2 Vols.) The various procedures are based on an evaluation of actual, forecast, or climatic soundings or on assumed model-atmospheric soundings. AWS has published a version of the Skew-T chart (DOD WPC-9-16-2) with a refractivity overprint. The construction and use of this chart was first described in AWS TR 169.

8.6. Fog Forecasting. The general aspects of fog forecasting are discussed in AWSM 105-44, as well as in standard textbooks of synoptic and applied meteorology. Certain specialized techniques require a detailed analysis of the lower level of the atmosphere sounding. Some objective fog-forecast techniques using sounding-derived parameters are listed in AWSTR 105-19 and AWSP 0-13.

8.7. Density Altitude. A version of the Skew-T chart with an overprint grid to facilitate computation of density altitude was published in AWS TR 105-101 (Rev. 2); individual copies of this chart can be requisitioned from AWS. For operations at remote sites where soundings and observations are not available, use the special nomogram and tables in AWS TR 165.

8.8. Cirrus Cloud. Techniques for forecasting cirrus on the basis of lapse-rate parameters are summarized in AWS TR 105-130. However, other approaches described in the same report appear to be more successful.

8.9. Maximum Temperature Forecasting. Various objective methods for forecasting maximum temperature have been described in the literature (see U. S. W. B. Forecasting Guide No. 4). Most of these techniques involve a procedure for evaluating the solar energy input at the surface either by subjective synoptic considerations or by a physical approach. In either case, the Skew-T chart or a similar diagram is frequently used to convert the energy input into temperature gain. This conversion is facilitated by overlaying a set of parallel lines representing energy units and reading off corresponding temperatures on the Skew-T chart, adiabatic chart, or tephigram. Myers has devised an overlay for the Weather Bureau Adiabatic Chart (Mon. Wea. Rev., Vol 86, 1958, pp. 149-164) and Kagawa has developed an overlay for the Canadian tephigram (DOT Canada, Met. Branch Tech Memo #683). A similar overlay can be prepared for the Skew-T chart.

8.10. Clouds. Use of adiabatic charts to estimate or forecast convective cloud amount, height, or intensity has been the subject of experiment for many years. In almost all this work it was necessary to adjust the procedure to local conditions, particularly as to place and time of soundings available, choice of representative surface temperature and moisture values, allowance for entrainment, and diurnal effects of convective mixing, topography, etc. Any success is usually attributed to the experimenter's experience and skill in such empirical modifications. One important difficulty is that in warm moist air masses small errors of several hundred feet in estimating or forecasting the height of the condensation level leads to very large differences in the forecast of cloud-top height, cloud coverage, and severity of associated convection weather. Recent literature on attempts to develop physical cumulus-cloud-development models (for computer evaluation) and direct observations of cumulus structure, dynamics, and evolution by aircraft and radar suggest more realistic and sophisticated procedures for modifying parcel analysis on adiabatic charts. Studies of cloud populations over large areas also provide the background for better cloud forecasting with parcel analysis by allowing area probability considerations to be introduced.

RUSSELL K. PIERCE, JR., *Major General, USAF*
Commander

CHARLES W. TIEMANN
Director of Administration

DISTRIBUTION: X

Hq AWS	80
Wgs, Gps	10
Sqs	5
Dets	2
ANG Wea Flts	2
MAC (MADDAPM)	2
Special	

4 Attachments
1. A Study of the Interpretation of Cloud Layers from Soundings
2. A Mathematical Analysis of Lapse-Rate Changes
3. References
4. Index of Terms and Concepts

Summary of Revised, Deleted, or Added Material

Manual has been generally updated and minor errors corrected. Chapter 3 has been revised; and Chapter 8, containing a discussion on forecasting uses of raobs with adiabatic charts, has been added.

A STUDY OF THE INTERPRETATION OF CLOUD LAYERS FROM SOUNDINGS

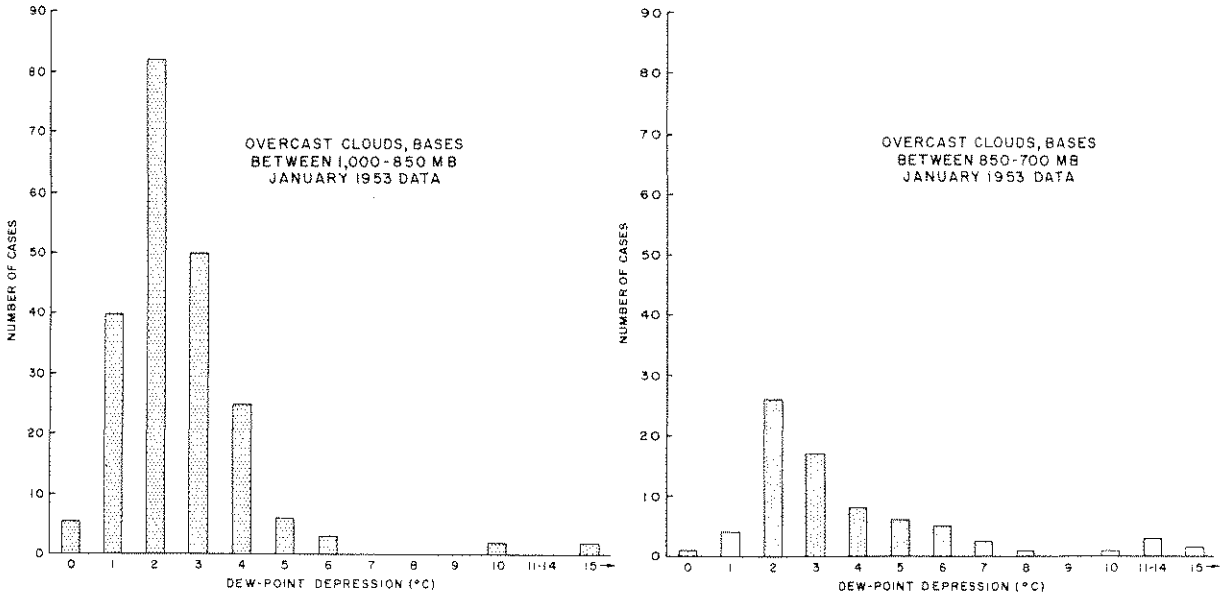

Figure 65. Frequency of Dew-Point Depressions (°C) at the Cloud Base for Solid Overcasts with Bases Between 1000 mb and 700 mb.

In an unpublished study conducted by Romo at Hq AWS, raobs for January 1953 from 29 U. S. Weather Bureau stations were compared with the lowest-cloud-layer observations at the location and time of each sounding. Only reliable cloud observations were used, e.g., only those of the lowest observed cloud layer and those obtained from available pilot reports. The T_d value reported on the sounding at the base of the lowest cloud layer was then recorded for each cloud observation. For example, if Pittsburgh reported an overcast at 4000 feet at 0330Z, the 0300Z Pittsburgh sounding was examined for the dew-point depression at that height above the surface. To compensate for the probable lag in the humidity element, the smallest dew-point depression within the first 1000 feet above the reported cloud-base height was selected as representative.

Bargraphs showing the frequency of the January 1953 reports with the various dew-point depressions at the base of solid overcasts are shown in Figure 65.

One graph refers to the base of the overcasts observed within the 1000- to 850-mb layer, while the other refers to overcast cloud bases in the 850- to 700-mb layer. The graphs show that dew-point depressions of 1°C to 4°C are typical of overcast cloud decks in both layers during January. In these graphs the few cases of dew-point depressions greater than 5°C are attributed to either instrument failure or transmission errors.

Figure 66 shows the frequencies of various dew-point depressions at the cloud-layer base for both 1/10 to 3/10 and 4/10 to 7/10 cloud coverages, which are further subdivided into the 1000- to 850-mb and 850- to 700-mb layers.

Again, the greatest concentration is around a dew-point depression of 2°C to 3°C at the cloud base; but the 850- to 700-mb reports show a more even distribution.

Figure 67 shows the dew-point depressions at the 850-, 700-, and 600-mb surfaces when clear skies occur. As expected, clear skies

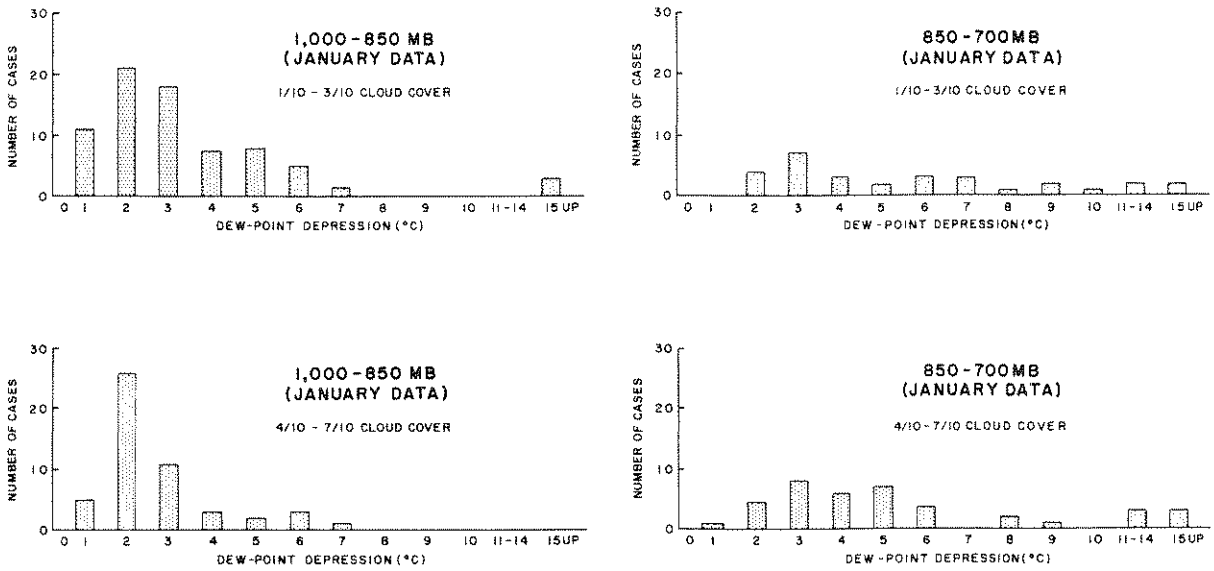

Figure 66. Frequency of Dew-Point Depressions (°C) at Cloud Base in 1/10 to 3/10 and 4/10 to 7/10 Cloud Layers Between 1000 mb and 700 mb.

are generally associated with much bigger dew-point depressions.

The data from Figures 65, 66, and 67, can be summarized in a different way. Figure 68 (from which Figure 63 of the text was derived) shows the percent probability for clear, scattered, broken, and overcast cloud conditions in January as a function of the dew-point depression at the cloud base for the 1000- to 850-mb and 850- to 700-mb layers. These data represent 1027 individual January observations, enough to indicate the order of magnitude of the dew-point depressions at the base of winter cloud layers; but these observations are not numerous enough to specify the actual percentages.

The above values are applicable during the winter months regardless of the synoptic situation. Given a sounding, one can determine from the graph the approximate probability of different sky-cover cloud layers with bases between 1000 mb and 600 mb for the layers of minimum dew-point depression up to 600 mb. During the warmer months of the year, the given probabilities are expected to increase for the smaller dew-point depressions and decrease for the larger depressions.

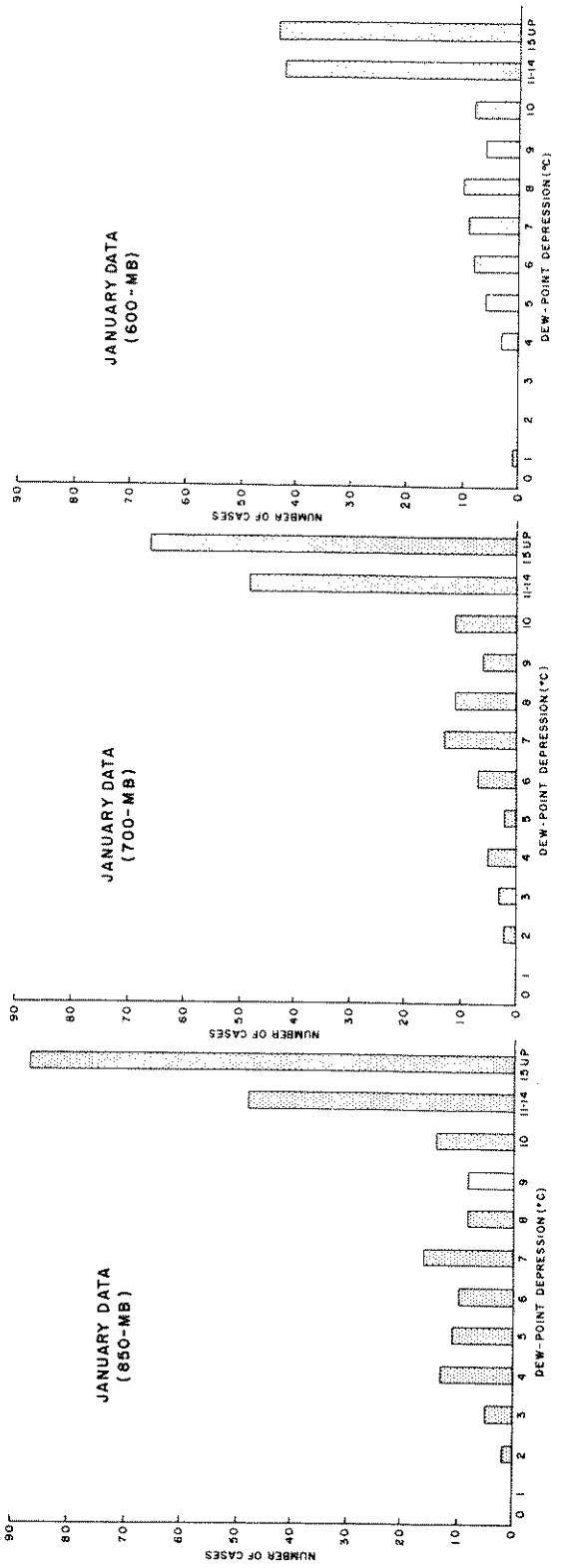

Figure 67. Dew-Point Depressions at 850-, 700-, and 600-mb Surfaces with Clear Skies.

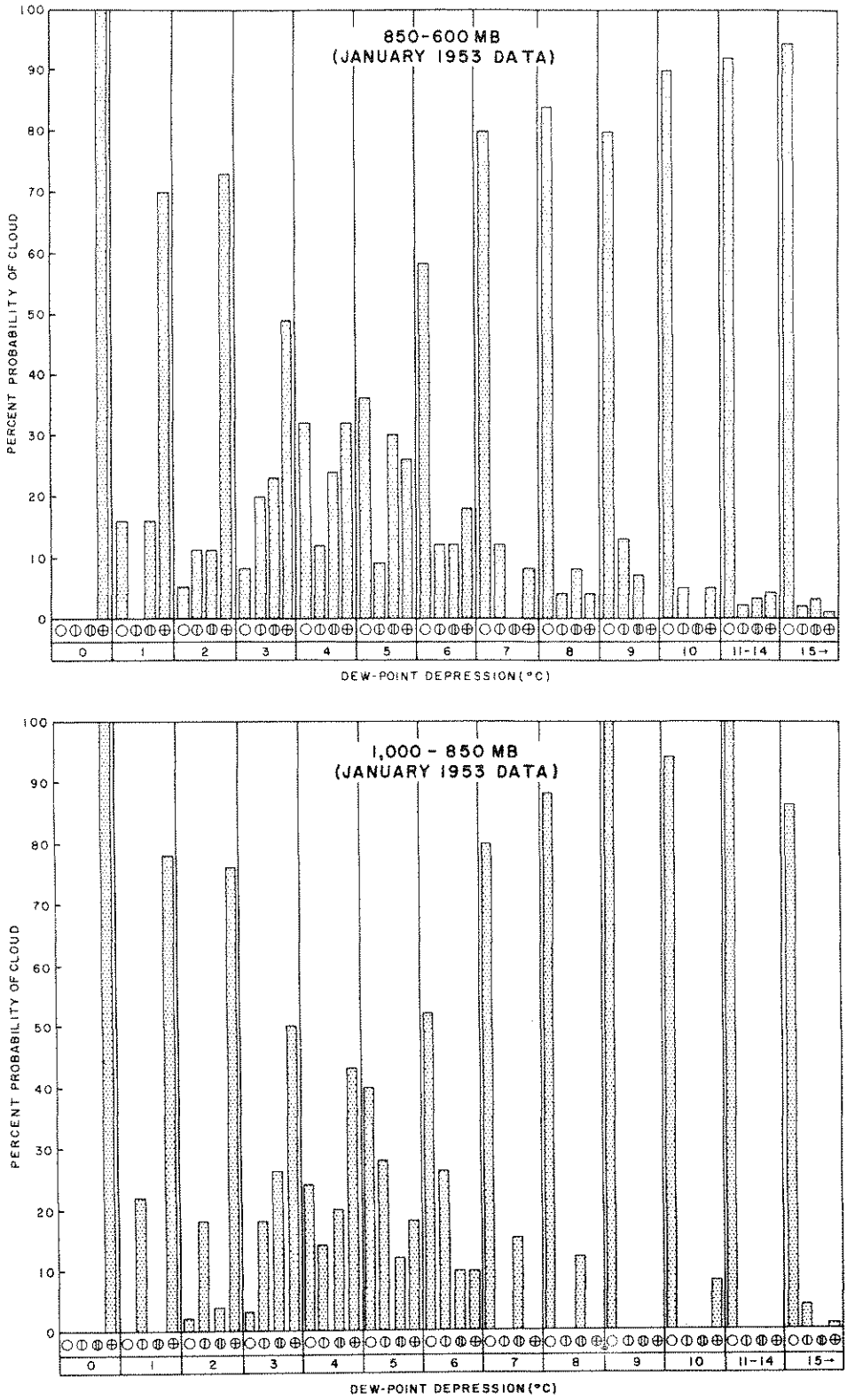

Figure 68. The Approximate Percent Probability of Different Sky Coverages with Cloud Bases Between 1000 and 850 mb, and 850 and 600 mb Plotted Against the Dew-Point Depression at the Cloud Base.

$\frac{d\gamma}{dt} = \frac{\partial \gamma}{\partial t} + \mathbf{v} \cdot \nabla \gamma$

A MATHEMATICAL ANALYSIS OF LAPSE-RATE CHANGES

In an unpublished study (on file in Hq AWS), Johannessen mathematically described the processes in the atmosphere that lead to a change in the lapse rate at a station.

Denoting the lapse rate by:

$$\gamma = - \frac{\partial T}{\partial z} \tag{1}$$

where T is temperature and z is height above the ground, we can write the identity:

$$\frac{\partial \gamma}{\partial t} \equiv \frac{\partial}{\partial t} \left(- \frac{\partial T}{\partial z} \right) \equiv - \frac{\partial}{\partial z} \left(\frac{\partial T}{\partial t} \right)$$

$$= - \frac{\partial}{\partial z} \left(\frac{dT}{dt} - \mathbf{v} \cdot \nabla T + w \gamma \right) \tag{2}$$

where $\mathbf{v}$ is the horizontal wind vector and w is the vertical motion.

From the first law of thermodynamics:

$$\frac{dQ}{dt} = c_p \frac{dT}{dt} - \alpha \frac{dp}{dt} \tag{3}$$

where Q is heat supplied to a mass unit of air, c_p is specific heat, α is specific volume, and p is pressure. In the atmosphere we can further write with sufficient accuracy (after considering the magnitude of the various terms in the expansion of $\frac{dp}{dt}$):

$$\frac{dp}{dt} \approx w \frac{\partial p}{\partial z} = - wg\rho \tag{4}$$

where p is density and g acceleration of gravity. Applying Equations (4) and (3) into (2) results in:

$$\frac{\partial \gamma}{\partial t} = - \frac{\partial}{\partial z} \left[\frac{1}{c_p} \frac{dQ}{dt} - \mathbf{v} \cdot \nabla T - w (\Gamma - \gamma) \right] \tag{5}$$

where we have written:

$\Gamma = g/c_p = 0.01\ ^\circ\text{C m}^{-1}$ = dry adiabatic lapse rate.

In Q above is included the latent heat exchanged during condensation and evaporation. If we want to exclude the latent heat from Q and let Q stand only for heat transfers by radiation and turbulence, we may do so by interpreting Γ as the saturation adiabatic lapse rate during the condensation phase, but as the dry adiabatic lapse rate otherwise.

Writing Equation (5) down, term by term (after performing the indicated differentiations of products):

$$\frac{\partial \gamma}{\partial t} = \begin{cases} \text{increasing stability when} < 0 \\ \text{decreasing stability when} > 0 \end{cases}$$

$$= - \frac{1}{c_p} \frac{\partial}{\partial z} \left(\frac{dQ}{dt} \right) : \begin{cases} \text{differential heating in the} \\ \text{vertical} \end{cases}$$

$$- \mathbf{v} \cdot \nabla \gamma \quad : \begin{cases} \text{advection of air of different} \\ \text{stability} \end{cases}$$

$$+ \frac{\partial \mathbf{v}}{\partial z} \cdot \nabla T \quad : \begin{cases} \text{shearing advection of} \\ \text{different temperature} \end{cases}$$

$$+ \frac{\partial w}{\partial z} (\Gamma - \gamma) \quad : \begin{cases} \text{shrinking and stretching of} \\ \text{column} \end{cases}$$

$$- w \frac{\partial \gamma}{\partial z} \quad : \begin{cases} \text{vertical advection of lapse} \\ \text{rate} \end{cases}$$

From "Use of the Skew T, log P diagram in analysis and forecasting" Air Force Manual, 1969.

A brief discussion of each term follows:

a. $-\frac{1}{c_p}\frac{\partial}{\partial z}\left(\frac{dQ}{dt}\right)$: This very important term is responsible for the pronounced diurnal change in lapse rate. By day, insolation heats the ground layers more than the layers above, thus $\frac{\partial}{\partial z}\left(\frac{dQ}{dt}\right)$ is negative and the whole term is positive; i.e., destabilization occurs. This effect may also be of importance away from the ground, e.g., night cooling from the top of cloud layers may destabilize the cloud tops and cause them to grow upwards. This effect has been offered as an explanation for nocturnal thunderstorms.

b. $-\mathbf{v}\cdot\nabla\gamma$: When a gradient of lapse rate exists and the wind blows across the isolines of lapse rate, air of a different lapse rate is simply replacing the air *in situ* and a corresponding change takes place. This process cannot, for instance, create an area of instability where none existed before. The process can merely translate already existing areas of stability and instability. However, it is one of the main effects to watch for on the map, since, for example, showers may occur as air of less stability is moving into an area.

c. $\frac{\partial \mathbf{v}}{\partial z}\cdot\nabla T$: The shearing advection process is identically zero if the winds are geostrophic, since $\frac{\partial \mathbf{v}_g}{\partial z} \sim \mathbf{k}\times\nabla T$ and $\mathbf{k}\times\nabla T\cdot\nabla T \equiv 0$.

Hence, if we write: $\mathbf{v} = \mathbf{v}_g + \mathbf{v}_a$, where $\mathbf{v}_g$ is the geostrophic wind, then $\frac{\partial \mathbf{v}}{\partial z}\cdot\nabla T = \frac{\partial \mathbf{v}_a}{\partial z}\cdot\nabla T$; i.e., only the *ageostrophic* wind components accomplishes anything. This term may create areas of instability where none existed before and may thus have greater prognostic importance if it can be evaluated properly by chart methods.

d. $\frac{\partial w}{\partial z}(\Gamma-\gamma)$: This process stabilizes a shrinking column and destabilizes a stretching column. A stretching column may, for instance, be one where the top ascends more rapidly than the bottom, hence, the top will cool more rapidly than the bottom and result in less stability. In a shrinking column, the top may ascend more slowly than the bottom and result in increased stability.

e. $-w\frac{\partial \gamma}{\partial z}$: This effect is a shifting up or down of existing lapse rates along the vertical. An example is that subsidence may spread stable inversion lapse rates downwards, almost to the ground in extreme cases.

The analysis above is a mental exercise that may be considered necessary to understand the way radiation, turbulence, release of latent heat, advection, shearing motion, and stretching and shrinking of atmospheric air columns contribute to changing the local lapse rate. At times one of the effects may be dominant to the extent that the other effects are only feeble reflex processes of smaller magnitude. In such cases the sign of the total is at least easy to determine. At other times, two or more of the processes are of the same and considerable magnitude but opposite sign so that the outcome may be hard to guess.

REFERENCES

[1] Albert, E. G.: "A Case Study of the Tropopause," Science Report #6, Contract No. AF 19(604) - 1755, New York Univ., Dept. of Met., 1959.

[2] Anon: "Forecasting Tornadoes and Severe Thunderstorms," Forecasting Guide No. 1, US Weather Bureau, September 1956, 34 pp.; see also, Galway, J. G.: "The Lifted Index as a Predictor of Latent Instability," Bull. Amer. Met. Soc., Vol. 37, No. 10, December 1956, pp. 528-529.

[3] Anon: "Testing a Thunderstorm Forecasting Method," AWS Bulletin, November 1952, pp. 24-27.

[4] Anon: "Theta-E Charts and Thunderstorm Forecasting," AWS Bulletin, No. 3, 1950, pp. 25-27.

[5] Austin, J. M., and Blackmer, R. H.: "The Variability of Cold Front Precipitation," MIT, Dept. of Met., Research Report #27, Contract Report No. DA-36-039SC-71136, July 1956.

[6] AWSM 105-44: "General Aspects of Fog and Stratus Forecasting," April 1954 (AD-33689).

[7] AWS TR 105-86: "Tropopause Analysis and Forecasting," March 1952 (ATI-162082).

[8] Banerji, S.: "Forecasting Thunderstorms at Nagpur by Slice Method," Indian Jn. of Met. and Geophys., Vol. 1, No. 3, July 1950, pp. 184-189.

[9] Bannon, J. K.: "An Analysis of Humidity in the Upper Troposphere and Lower Stratosphere," MRP 563, May 1950 (ATI-88400).

[10] Bannon, J. K., Frith, R., and Shellard, H. C.: "Humidity of the Upper Troposphere and Lower Stratosphere Over Southern England," Geophysical Memoirs No. 88, Met. Office, London, 1952.

[11] Bellamy, J. C.: "Objective Calculations of Divergence, Vertical Velocity and Vorticity," Bull. Amer. Met. Soc., Vol. 30, No. 2, February 1949, pp. 45-49.

[12] Bergeron, T.: "The Physics of Fronts," Bull. Amer. Met. Soc., Vol. 18, No. 9, September 1937, pp. 265-275.

[13] Berry, F. A., Jr., Bollay, E., and Beers, N. R.: Handbook of Meteorology, 1st Edition, McGraw-Hill Book Co., Inc., New York, 1945.

[14] Bjerknes, J.: "Saturated-Adiabatic Ascent of Air Through Dry-Adiabatically Descending Environment," Quart. Jn. Roy. Met. Soc., Vol. 64, 1938, pp. 325-330.

[15] Bjerknes, J., and Holmboe, J.: "On the Theory of Cyclones," Jn. of Met., Vol. 1, Nos. 1-2, September 1944, pp. 1-22, plus Figures 9, 10, 14, 15, and 16.

[16] Braham, R. R., Jr., and Draginis, M.: "Roots of Orographic Cumuli," 1st Conference on Cumulus Convection, May 19-22, 1959, 14 pp., plus figures.

[17] Bunker, A. F.: "On the Determination of Moisture Gradients from Radiosonde Records," Bull. Amer. Met. Soc., Vol. 34, No. 9, November 1953, pp. 406-409.

[18] Byers, H. R., and Braham, R. R.: The Thunderstorm, Report of the Thunderstorm Project, U.S. Dept. of Commerce, US Weather Bureau, GPO, June 1949.

[19] Conover, J. H., and Wollaston, C. H.: "Cloud Systems of a Winter Cyclone," Jn. of Met., Vol. 6, 1949, pp. 249-260.

[20] Cressman, G. P.: "An Approximate Method of Divergence Measurement," Jn. of Met., Vol. 11, No. 2, April 1954, pp. 83-90.

[21] Cressman, G. P.: "The Influence of the Field of Horizontal Divergence on Convective Cloudiness," Jn. of Met., Vol. 3, No. 3, September 1946, pp. 85-88.

[22] Curtis, R. C., and Panofsky, H. A.: "The Relation Between Large-Scale Vertical Motion and Weather in Summer," Bull. Amer. Met. Soc., Vol. 39, No. 10, October 1958, pp. 521-531.

[23] Danielsen, E. F.: "The Laminar Structure of the Atmosphere and Its Relation to the Concept of a Tropopause," PhD Thesis, Univ. of Washington, Dept. of Met. and Clim., 1958, 106 pp.; also reprint from Arch. Met. Geoph. Biokl., Serier A, Vol. 11, No. 3, 1959, pp. 293-332.

[24] Endlich, R. M., and McLean, G. S.: "The Structure of the Jet Stream Core," Jn. of Met., Vol. 14, No. 6, December 1957, pp. 543-552.

[25] Fawbush, E. J., and Miller, R. C.: "A Method for Forecasting Hailstone Size at the Earth's Surface," Bull. Amer. Met. Soc., Vol. 34, No. 6, June 1953, pp. 235-244.

[26] Godson, W. L.: "Superadiabatic Lapse Rate in the Upper Air," Tech. Note No. 16, WMO, Geneva, 1955.

[27] Godson, W. L.: "Synoptic Properties of Frontal Surfaces," Quart. Jn. Roy. Met. Soc., Vol. 77, No. 334, October 1951, p. 641.

[28] Graham, R. D.: "A New Method of Computing Vorticity and Divergence," Bull. Amer. Met. Soc., Vol. 34, No. 2, February 1953, pp. 68-74.

[29] Graves, M. E.: "The Relation Between the Tropopause and Convective Activity in the Subtropics (Puerto Rico)," Bull. Amer. Met. Soc., Vol. 32, No. 2, February 1951, pp. 54-60.

[30] Herlofson, N.: "The T, log p — Diagram with Skew Coordinate Axes," Meteorologiske Annaler, Vol. 2, No. 10, Oslo, 1947, pp. 311-342 plus diagrams.

[31] Hewson, E. W.: "The Application of Wet-Bulb Potential Temperature to Air Mass Analysis," Quart. Jn. Roy. Met. Soc., Vol. 63, No. 266, July 1936, pp. 387-420; see also, Quart. Jn. Roy. Met. Soc., Vol. 63, No. 268, January 1937, pp. 7-30; and Quart. Jn. Roy. Met. Soc., Vol. 63, No. 271, July 1937, pp. 323-337.

[32] Hodge, M. W.: "Superadiabatic Lapse Rates of Temperature in Radiosonde Observations," Mon. Wea. Rev., Vol. 84, No. 3, March 1956, pp. 103-106.

[33] Holmboe, J., Forsythe, G. E., and Gustin, W.: Dynamic Meteorology, John Wiley and Sons, Inc., New York, 1945.

[34] James, D. G.: "Investigations Relating to Cirrus Cloud," MRP 933, September 1955; see also Met. Mag., Vol. 86, No. 1015, January 1957, pp. 1-2; and Met. Mag., Vol. 88, No. 1041, March 1959, pp. 79-80.

[35] Local Forecast Study for Wright-Patterson AFB: "Thunderstorms and Rain Showers," Terminal Forecast Manual, Section IV A, typescript, 14 November 1956 (AD-116123).

[36] Ludlam, F. H., and Mason, B. J.: "Radar and Synoptic Studies of Precipitating Clouds," Tech. Rept. No. 1, Contract No. AF 61(514)-809, Dept of Met., Imperial College of Science and Techn., January 1956, 44 pp.

[37] Malkus, J. S.: "On the Structure of the Trade Wind Moist Layer," Tech. Rept. No. 42, Ref. 57-9, Woods Hole Oceanographic Institute, January 1957, unpublished manuscript.

[38] Malkus, J. S.: "Recent Advances in the Study of Convective Clouds and Their Interaction with the Environment," Tellus, Vol. 4, No. 2, May 1952, pp. 71-87.

[39] Marshall, J. S.: "Effects of General Lifting or Subsidence on Convective Overturning," 1st Conference on Cumulus Convection, May 1959, Woods Hole, McGill Univ., Montreal, 1959, unpublished manuscript.

[40] Mason, B. J., and Howorth, B. P.: "Some Characteristics of Stratiform Clouds Over North Ireland in Relation to Their Precipitation," Quart. Jn. Roy. Met. Soc., Vol. 78, 1952, pp. 226-230.

[41] Matthewman, A. G.: "Cloud in Relation to Warm and Quasi-Stationary Fronts Near Bircham Newton in Winter," MRP 747, Met. Office., London, 1952.

[42] Matthewman, A. G.: "Studies of the Structure of Fronts," Part I, MRP 597, Met. Office, London, 1950.

[43] Murgatroyd, R. J., and Goldsmith, P.: "Cirrus Cloud Over Southern England," MRP 833, September 1953; (published later as) "High Cloud Over Southern England," Prof. Notes No. 119, Met. Office, London, 1956.

[44] Namias, J.: "Subsidence Within the Atmosphere," Harvard Meteorological Studie No. 2, 1934.

[45] Namias, J., et al.: "An Introduction to the Study of Air Mass and Isentropic Anal ysis," 5th Revised and Enlarged Edition, Amer. Met. Soc., October 1940.

[46] Normand, C. W. B.: "On Instability from Water Vapour," Quart. Jn. Roy. Met. Soc., Vol. 64, No. 273, January 1938, pp. 47-69.

[47] Petterssen, S.: Weather Analysis and Forecasting, McGraw-Hill Book Co., Inc., New York, 1940, p. 101.

[48] Petterssen, S.: Weather Analysis and Forecasting, 2d Edition, Vol. II, McGraw-Hill Book Co., Inc., New York, 1956.

[49] Petterssen, S., Knighting, E., James, R. W., and Herlofson, N.: "Convection in Theory and Practice," Geofysiske Publikasjoner, Vol. 16, No. 10, Oslo, 1946, 44 pp.

[50] Priestley, C. H. B.: "Buoyant Motion in a Turbulent Environment," Austr. Jn. of Phys., Vol. 6, No. 3, September 1953, pp. 279-290.

[51] Reihl, H.: Tropical Meteorology, McGraw-Hill Book Co., Inc., New York, 1954, pp. 53-70.

[52] Rossby, C. G.: "Thermodynamics Applied to Air Mass Analysis," papers in Oceanog. and Met., Woods Hole Oceanog. Instn., and MIT, Vol. 1, No. 3, 1932, 41 pp

[53] Sansom, H. W.: "A Study of Cold Fronts Over the British Isles," Quart. Jn. Roy. Met. Soc., Vol. 77, No. 331, January 1951, pp. 96-120.

[54] Saunders, P. M.: "The Thermodynamics of Saturated Air: A Contribution of the Classical Theory," Quart. Jn. Roy. Met. Soc., Vol. 83, No. 357, July 1957, pp. 342-350; also Ludlam, F. A., and Saunders, P. M.: "Shower Formation in Large Cumulus," Tellus, Vol. 8, No. 4, November 1956, pp. 424-442.

[55] Sawyer, J. S.: "Effect of Atmospheric Inhomogeneity on the Interpretation of Vertical Temperature Soundings," Met. Mag., Vol. 82, No. 975, September 1953, pp. 257-263.

[56] Sawyer, J. S.: "The Free Atmosphere in the Vicinity of Fronts, Analysis of Observations by the Meteorological Research Flight," MRP 807, Met. Office, London, 1953: (published later as) "The Free Atmosphere in the Vicinity of Fronts," Geophysical Memoirs #96, Met. Office, London, 1955.

[57] Sawyer, J. S., and Dinsdale, F. E.: "Cloud in Relation to Active Warm Fronts Near Bircham Newton During the Period April 1942 — April 1946," MRP 799, Met. Office, London, 1953.

[58] Showalter, A. K.: "A Stability Index for Thunderstorm Forecasting," Bull. Amer. Met. Soc., Vol. 34, No. 6, June 1953, pp. 250-252.

[59] Similä, A.: "Die Aerologischen Gewittertendenzkarten," Tellus, Vol. 1, No. 4, November 1949, pp. 18-23.

[60] Smithsonian Meteorological Tables, 6th Revised Edition, Smithsonian Institute, Washington, D. C., 1951, p. 352.

[61] Wagner, A. J., and Sanders, F.: "Some Relationships Between Air Mass Stability, Large-Scale Vertical Motion and Thunderstorm Frequency," Appendix 2 to "Some Application of Dynamical Concepts," MIT, Dept. of Met., Final Report on Contract No. AF 19(604)-1305, February 28, 1959, pp. 53-71 (AD-212267).

[62] Wexler, A.: "Low-Temperature Performance of Radiosonde Electric Hygrometer Elements," Jn. Res. Nat. Bur. Stand., Vol. 43, 1949, pp. 49-56.

[63] Wexler, H.: "The Cooling in the Lower Atmosphere and the Structure of Polar Continental Air," Mon. Wea. Rev., Vol. 64, No. 4, April 1936, pp. 122-136.

[64] Wexler, R., Reed, R. J., and Honig, J.: "Atmospheric Cooling by Melting Snow," Bull. Amer. Met. Soc., Vol. 35, No. 2, February 1954, pp. 48-51.

[65] WMO: Technical Regulations, Vol. I, WMO-No. 49, BD2, Secretariat of World Meteorological Organization, Geneva, 2d Edition, 1959.

INDEX OF TERMS AND CONCEPTS

(Shows paragraph where certain terms and concepts are defined, introduced, or primarily discussed.)

MAC—S AFB, Ill 69-6627